BRNO UNIVERSITY OF TECHNOLOGY
VYSOKÉ UČENÍ TECHNICKÉ V BRNĚ

FACULTY OF MECHANICAL ENGINEERING
FAKULTA STROJNÍHO INŽENÝRSTVÍ

ENERGY INSTITUTE
ENERGETICKÝ ÚSTAV

VIZUALIZATION OF LIQUID BREAK-UP FROM ATOMIZATION NOZZLES
VIZUALIZACE ROZPADU KAPALINY U ROZPRAŠOVACÍCH TRYSEK

BACHELOR'S THESIS
BAKALÁŘSKÁ PRÁCE

AUTHOR — **Lada Janáčková**
AUTOR PRÁCE

SUPERVISOR — **doc. Ing. Jan Jedelský, Ph.D.**
VEDOUCÍ PRÁCE

BRNO 2016

VYSOKÉ UČENÍ TECHNICKÉ V BRNĚ
FAKULTA STROJNÍHO INŽENÝRSTVÍ

Zadání bakalářské práce

Ústav:	Energetický ústav
Studentka:	**Lada Janáčková**
Studijní program:	Strojírenství
Studijní obor:	Základy strojního inženýrství
Vedoucí práce:	**doc. Ing. Jan Jedelský, Ph.D.**
Akademický rok:	2015/16

Ředitel ústavu Vám v souladu se zákonem č.111/1998 o vysokých školách a se Studijním a zkušebním řádem VUT v Brně určuje následující téma bakalářské práce:

Vizualizace rozpadu kapaliny u rozprašovacích trysek

Stručná charakteristika problematiky úkolu:

Vizualizační metody umožňují získat kvalitativní i kvantitativní informace o mnoha dějích. Zde je plánována dokumentace vývoje spreje tvořeného tlakovou rozprašovací tryskou pomocí makrofotografie s využitím DSLR fotoaparátu, příp. vysokorychlostní kamery. Bude studován zejména primární rozpad kapaliny. Obrazy spreje budou upraveny ve vhodném programovém prostředí. Fotogrammetrická analýza obrazu umožní získat informace o struktuře a geometrii spreje, velikosti a tvaru generovaných kapek apod.

Cíle bakalářské práce:

1. rešerše vizualizačních metod používaných ve sprejích, popis používaných typů konfigurací, zhodnocení jejich možností a výhod
2. typické struktury ve spreji (kapalné filmy, provazce, kapky a jejich shluky), popis rozptylu světla na těchto strukturách a důsledky pro vizualizační experimenty
3. příprava a sestavení vizualizačního řetězce (objekt, zdroj světla, kamera/fotoaparát, příp. další optické prvky)
4. optimalizace nastavení vizualizačního řetězce pro konkrétní případ tlakové vířivé trysky
5. provedení sady vizualizačních experimentů (zaměření na primární rozpad a vývoj kapalného filmu, příp. na sekundární breakup, dokumentace experimentu
6. postprocesing obrazových dat pomocí vhodného programového vybavení
7. fotogrammetrická analýza obrazu, fyzikální popis získaných výsledků a závěry s ohledem na zkoumaný objekt

Seznam literatury:

SMITS, A. J. a LIM, T. T. Flow Visualization: Techniques and examples. London: Imperial College Press, 2003. ISBN 1-86094-193-1.

Lefebvre AH. Atomization and sprays. Combustion, vol. xi. New

York: Hemisphere Pub. Corp.; 1989. p. 421.

ĎURDINA, L. Metody vizualizace proudění. Brno: Vysoké učení technické v Brně, Fakulta strojního inţenýrství, 2010. 45 s.

S.N. Sridhara and B.N. Raghunandan / JAFM, Vol. 3, No. 2, pp. 111-123, 2010.

Seoksu Moon, Choongsik Bae, Essam F. Abo-Serie, Jaejoon Choi, Internal and near-nozzle flow of a pressure-swirl atomizer under varied fuel temperature, ATOMIZATION AND SPRAYS 17(6):529-550 · JANUARY 2007, · DOI: 10.1615/AtomizSpr.v17.i6.30

Termín odevzdání bakalářské práce je stanoven časovým plánem akademického roku 2015/16

V Brně, dne

L. S.

doc. Ing. Jiří Pospíšil, Ph.D. ředitel ústavu	doc. Ing. Jaroslav Katolický, Ph.D. děkan fakulty

Abstract

In the field of experimental fluid mechanics, visualizations play an important role. The images give an insight into the principal of fluid behavior and help with understanding of physical processes in flows in general. This thesis deals with visualization of liquid breakup from atomization nozzles.

The thesis describes fundamentals of liquid atomization, as techniques for spray visualization. Further in this work an analysis of elements in the visualization techniques are discussed and tested experimentally. Laboratory tests were performed using small pressure-swirl atomizer originally designed for the combustion of kerosene in turbojet aircraft engine and a part of the experiments was carried out at a pressure spiral atomizer. The thesis documents the influence of the light source to image quality. Moreover, spray behavior is analysed using macro-photography with focus on primary breakup which plays major role in the whole process of the spray formation and spray characteristics.

Keywords: Flow visualization, visualization techniques, atomization, liquid breakup, pressure-swirl atomizer, spiral atomizer, spray characteristics.

Abstrakt

V oblasti mechaniky tekutin hraje vizualizace významnou roli. Fotografie poskytují vhled do zásad chování tekutin a obecně pomáhají k lepšímu pochopení fyzikálních procesů proudění. Tato práce se zabývá vizualizací rozpadu kapalin u rozprašovacích trysek.

Práce popisuje základy rozpadu kapalin, stejně jako metody pro vizualizaci. Dále je v práci probrána a experimentálně testována analýza prvků ve vizualizačních metodách. Laboratorní testy byly provedeny na malé tlakové vířivé trysce určené pro spalování kerosinu v proudovém leteckém motoru a část experimentů byla provedena na tlakové spirálové trysce. Práce dokumentuje vliv zdroje světla na kvalitu fotografie. Chování spreje je navíc analyzováno pomocí makrofotografie se zaměřením na primární rozpad, který hraje hlavní roli v celém procesu tvorby spreje a sprejových charakteristik.

Klíčová slova: Vizualizace proudění, vizualizační metody, atomizace, rozpady kapaliny, tlaková vířivá tryska, spirálovitá tryska, charakteristiky spreje.

Bibliographic citation

JANÁČKOVÁ, L. *Vizualizace rozpadu kapaliny u rozprašovacích trysek.* Brno: Vysoké učení technické v Brně, Fakulta strojního inženýrství, 2016. 60 s. Vedoucí bakalářské práce doc. Ing. Jan Jedelský, Ph.D.

Affirmation

I declare that this bachelor's thesis is the result of my own work led by doc. Ing. Jan Jedelský, Ph.D. and all used sources are duly listed in the bibliography.

Lada Janáčková

Acknowledgments

Foremost, I would like to express my sincere gratitude to my supervisor doc. Ing. Jan Jedelský, Ph.D. for his guidance, patience, motivation nad his willingness to help me with problems I was facing.

I am also thankful that I had the opportunity to create this work with the support of the project no. GA15-09040S funded by the Czech Science Foundation and LO1202 NETME CENTRE PLUS funded by the Ministry of Education, Youth and Sports of the Czech Republic under the National Sustainability Programme I.

I would like to express my thanks to Bc. Milan Malý who helped me with the preparation of measurement and taught me whole year how to work in the laboratory. My thanks also belongs to Ph.D. student Ing. Matouš Zaremba for his valuable advices and comments during writing this thesis.

Last, but not least, I would like to thank my family, especially my parents, for the support they have provided me throughout my entire study.

Introduction

Devices designed for spraying a liquid i.e. atomizers are common in many industrial applications. During the past many different designs of atomizers were developed. The examination of the atomizers, consequently spray properties, was done by means of the spray visual observations, laser anemometry and other non-intrusive techniques. Especially the visualization techniques plays major role in the field of experimental fluid mechanics due to their advantages: simple and relatively cheap price, non-intrusive or broad range of post-processing options.

Capturing of detailed images of the spray structure allows better understanding of fluid flow behavior of the liquid breakup process and spray formation in general. Commonly studied parameters include primary and secondary atomization, spray cone angle, liquid sheet breakup length, the size and shape of generated droplets and liquid mass distribution in the spray. These aspects can be studied by several techniques such as Front lighting, Side lighting, Shadowgraphy, Schlieren, Holography, Particle Image Velocimetry (PIV) and planar Laser Induced Fluorescence (PLIF).

This thesis is focused on the description of the theory of visualization techniques used in sprays. Two of these techniques have been tested in a real application, namely shadowgraphy and side lighting technique.

At the beginning of the present work a theoretical background of the liquid atomization and visualization techniques are briefly described. In the practical part of this work the test conditions and experimental setup are present. At the end of the thesis results from experiments are discussed.

Figure 1-2, Figure 5-7 and Figure 5-8 were created in cooperation with Bc. Milan Malý and they are also used in his master thesis.

Contents

1 Liquid atomization

This chapter describes the basic aspects of the liquid breakup, i.e., liquid atomization. Firstly, aspects influencing atomization are described. Secondly, the basic mechanisms of liquid disintegration are studied.

1.1 Introduction

Atomization is a process in which liquid (fuel) is converted into small droplets by internal and external forces as a result of the interaction between liquid and surrounding air. [1]

The atomization process consists of two main areas – primary and secondary atomization, (see Figure 1-1). *Primary atomization* is situated closer to the exit orifice, where liquid stream is disintegrated into various liquid shreds, ligaments and large droplets by disruptive aerodynamic forces. Many of such resulting structures are unstable and undergo further disruption into smaller droplets. This process is called *secondary atomization* and it is located further downstream from the atomizer. [1, 2]

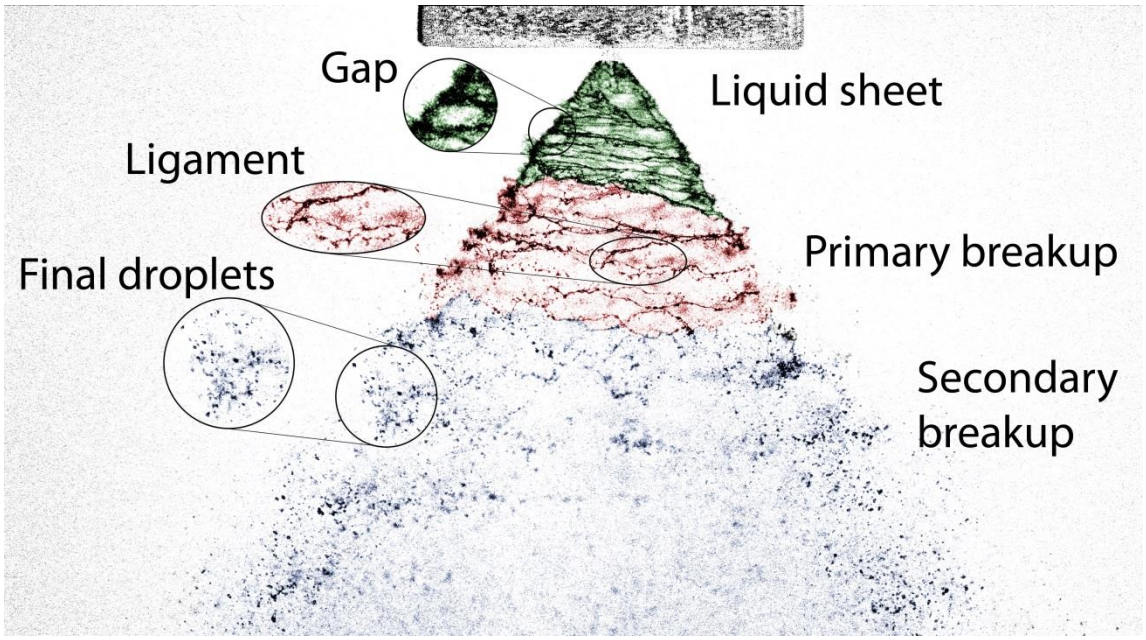

Figure 1-1 Primary and secondary atomization

1.2 Atomizers

The devices used for atomization of liquids are called atomizers. There are three main types of atomizers briefly described below.

Pressure atomizers

The most common type of atomizers is pressure atomizer. The pressure atomizers work on the basis of the conversion of pressure into kinetic energy, which results in high velocity between the liquid and the surrounding air. A simple construction, no additional input energy or a need of another medium are the main advantages of these devices. [3, 4]

Twin-fluid atomizers

There are two similar groups of twin-fluid atomizers – internal-mixing and external-mixing atomizers. They use the kinetic energy of the air stream to disintegrate liquid stream or sheet into ligaments and drops. The main advantages are good atomization at low pressure, the ability to atomize high-viscosity liquids, and larger exit orifice which is suited for contaminated liquids. [1, 5]

Other atomizers

Many other atomizers have been developed for the use in special cases. These includes rotary, electrostatic, ultrasonic, windmill atomizers, etc. These atomizers use mechanism of accelerated fluid, but more often is used a work of electromagnetic field, sound waves, mechanical disruption, etc. For detailed information the reader is referred to [2].

1.3 Liquid physical properties

The spray characteristics are strongly affected by the atomizer size and geometry, physical properties of atomizing liquid and ambient air. The most important liquid physical properties are density, viscosity and surface tension. [1, 2, 6]

1.3.1 Liquid density

Liquid density ρ_l is defined as liquid mass m per unit volume V:

$$\rho_l = \frac{m}{V} \tag{1.1}$$

The unit of density is kg/m^3. The density of liquid may be considered unchangeable in general, but that of a gas changes according to the pressure. Most commonly liquid is water with the density of 1000 kg/m³ at 4 °C and 0.1 MPa. [7] The main effect of liquid density is the production of a more compact and penetrating spray. [8]

1.3.2 Liquid viscosity

We recognize two types of viscosity. *Dynamic viscosity* can be describe as a ratio of the resistence of a fluid in motion against the acting stresses between neighboring particles. The relationship can be expressed by:

$$\tau = \mu \frac{du}{dy} \tag{1.2}$$

where τ is shear stress, μ is dynamic viscosity and $\frac{du}{dy}$ is derivative of velocity. This relation is known as Newton's law of viscosity, which applies to most liquid and gases.

More often can be used *kinematic viscosity*, which measures liquid resistance to flow under the influence of gravity. It is defined as:

$$\nu = \frac{\mu}{\rho_l} \tag{1.3}$$

where v is kinematic viscosity. The unit of dynamic viscosity is $Pa{\cdot}s$ and that of kinematic viscosity m^2/s. [7] According to Nabah [9], viscosity tends to inhibit the growth of instabilities and generally delays the liquid breakup.

1.3.3 Surface tension

Surface tension is defined as the force that resists the formation of new surface area. It is expressed as:

$$\sigma = \frac{F}{l} \tag{1.4}$$

where F is a force along the fluid surface and l is the length of the fluid surface. Besides, it can be also defined as ratio of the minimum energy required for atomization dE_A to the increase in surface area dA:

$$\sigma = \frac{dE_A}{dA} \tag{1.5}$$

The unit of this property is J/m^2. The liquid surface tension forces play an important role in the formation of a new surface. These forces determine whether the liquid sheet is going to breakup or remain stable. [9]

1.4 Liquid breakup

Disintegration of the liquid issuing from the atomizer is characterized by three distinct mechanisms, namely breakup of liquid stream, breakup of liquid sheet and breakup of droplet.

1.4.1 Breakup of liquid stream

Theoretical analysis of liquid stream instability was first made by Rayleigh [10]. He considered a simple case of a nonviscous liquid stream under laminar flow conditions. According to his findings, the liquid stream starts to run down from the exit orifice. The competitive environment on the surface of the stream between cohesive and disruptive forces causes formation of small oscillations. Amplifying the oscillations gives formation of a neck, which in turn becomes unstable and thinner and breaks down due to surface tension. The drops formed from the neck are usually nonspherical and coalesce into large drops with small „satellite“ drops between them. Rayleigh’s assumption of stream disintegration is shown in Figure 1-2. Later, Weber [11] extended Rayleigh‘s stability analysis incorporating the effect of viscosity. As it is pointed out in [8], Weber showed that the viscosity has a stabilizing effect that decreases the breakup rate and increases the size of droplets. Both of these studies imply that the entire disintegration process largely depends on the relative velocity between the liquid stream and the ambient air. According to Lefebvre [1], at low velocities, the droplets from the disintegrated stream have fairly uniform size and their diameters are nearly twice of the initial stream diameter. With increasing velocity is reduced the optimal wavelength for the disintegration of the liquid stream and the droplet diameter. For a very high velocities atomization occurs very close from the exit orifice.

An important parameter in analysis of fluid flows is Weber number, which is the relationship between the disruptive aerodynamic force and surface tension, defined as:

$$\mathrm{We} = \frac{\rho_l U_0^2 \mathrm{D}}{\sigma} \tag{1.6}$$

where *D* is droplet diameter and U_0^2 is droplet velocity before a collision. The higher the Weber number, the larger the deforming external pressure forces. When Weber number is high (at high velocities and pressures of liquid), breakup starts immediately at the exit orifice. This process is called *prompt atomization.* [1, 2]

More information about stream breakup length, types of stream disintegration, etc. are described in Agraval [12].

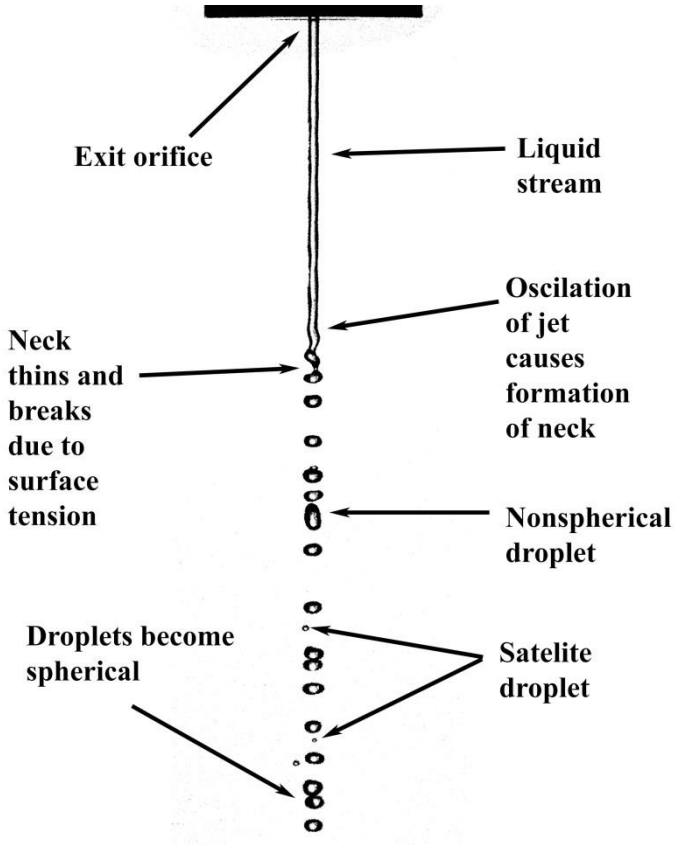

Figure 1-2 Liquid stream breakup

1.4.2 Breakup of liquid sheet

Most atomizers produce a conical or flat liquid sheet, rather than liquid stream. Formation of *conical* sheet is typical for the pressure-swirl atomizers. Liquid sheet instability is influenced mainly by its relative velocity, liquid properties, the ambient gas and thickness of liquid sheet. At low relative velocity is generated a wave motion on the sheet causing a formation of cylindrical ligaments, which breaks away from its edge and further disintegrates into drops of uniform size according to the Rayleigh mechanism, as shown in Figure 1-2. At high velocities atomization occurs at the exit orifice. [1, 2] Many studies have identified sheet instabilities and factors influencing liquid sheet breakup. According to Dabiri et al. [14], the main factor for breakup has occurrence of cavitation. Lin [15] conducted a detailed study of a viscous liquid sheet falling in gravity. For more information the reader is referred to [16].

According to Lefebvre [2], Fraser and Eisenklam in 1953 first described the breakup and droplet formation of *flat* sheet. They defined three distinct modes of sheet breakup – *rim*, *wave* and *perforated sheet*. Rim breakup is generated by acceleration forces on the outer edges of the sheet, which can destabilize a fluid-fluid interface. These disturbances are manifested as ripples, which turn into rapidly expanding holes that break down into ligaments and droplets. Later these three breakup modes were verified by a more detailed analysis by Altieri et al. [13]. They introduced the influence of liquid properties on the resulting atomization. In comparison to the single-phase emulsion (water) results showed that an oil phase causes earlier breakup of the sheet and larger droplets.

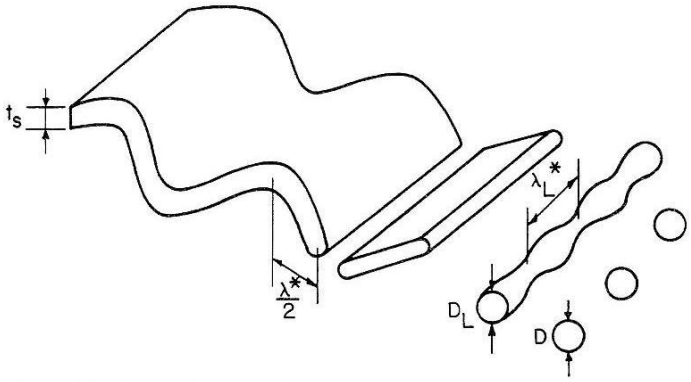

Figure 1-3 Breakup of liquid sheet

1.4.3 Breakup of droplet

The droplets from the liquid stream or sheet may disintegrate into multitude of smaller structures. This process belongs to secondary atomization, as already mentioned above.

In general, during flight through the air surface tension forces of a droplet increase until they exceed the stable maximum limit and the droplet disintegrates into smaller fragments. According to findings of Ashgriz [17], the most important parameter for the phenomenon of secondary atomization is the Weber number. In his study, the droplet breakup is characterized by a morphology consisting of the following modes: vibrational, bag, multimode, sheet-thinning, and catastrophic (see Figure 1-4). At very low We ($We \leq 11$) droplet breaks into several larger fragments. It is due to oscillations of the drop so called *vibrational mode*. With a higher We ($11 \leq We \leq 35$) *bag breakup* occurs, which is the most important mode, because minimal energy is needed. The drop becomes increasingly flattened and it is blown out into the form of a hollow bag attached to a roughly circular rim. The bag produces amount of very fine droplets and the rim breaks up into small number of larger drops. In case of *multimode breakup* ($35 \leq We \leq 80$), the drop is exposed to a fast airstream and is deformed in an opposite direction than in the bag breakup. The edges of the saucer shape are drawn out into a thin sheet and then into fine filaments witch breakup into drops. With increasing relative velocity the *sheet-thinning mode* occurs ($80 \leq We \leq 350$), which means that droplet boundaries becomes thinner and belongs to further breakup. After exceeding the critical We number ($We \geq 350$) occurs *catastrophic mode*. The droplet disintegrates into very small drops of various sizes, which is the final breakup.

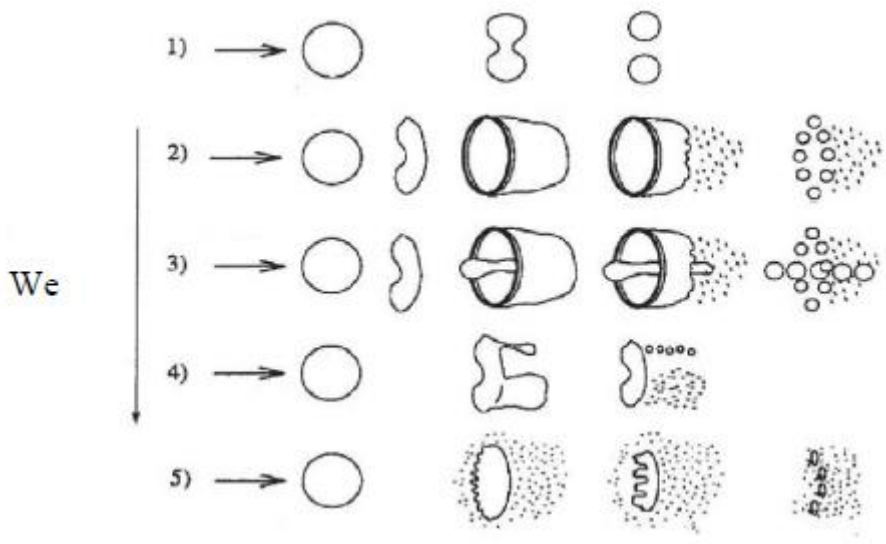

Figure 1-4 Different modes of droplet breakup – 1) vibrational, 2) bag, 3) multimode, 4) sheet-thinning, 5) catastrophic, adapted from [12]

2 Visualization techniques used in sprays

2.1 Introduction

The consolidated technique which analyses the behavior of the object invisible to the eye as image information is called *visualization*. It is applicable to various phenomena such as flow, heat, sound, chemical kinetics, electromagnetism, etc. [18] State of the object or even its temporal evolution, connection and the physical nature of observed phenomena can be studied using available *visualization techniques*. [19]

Basically, each visualization arrangement consists of a tested object (scattering particle), an illumination system (source of light) and a receiver (camera, etc.). As mentioned in [20], main features and benefits of the flow visualization are:

- good understanding of the flow structure,
- simple to use,
- cost effective.

In following subchapters is presented a summary of the visualization techniques used in the fluid mechanics. The aim is to provide an overview that encompasses the majority of the currently available methods. Summary of information obtainable from various visualization techniques in the spray field is presented in Tab. 2-1 at the end of this chapter.

2.2 Light scattering

For investigation of liquid breakup the visualization techniques are used, where the choice of illumination is very important. Light is defined as a progressive transverse electromagnetic wave. It is characterized by wavelength, defined as:

$$\lambda = \frac{c}{f} \tag{1.7}$$

where *c* is speed of light in vacuum and *f* is frequency of light. The human eye is able to detect electromagnetic waves with wavelengths of 390 nm – 790 nm. [21]

There are two main processes of light scattering – *elastic*, in which the wavelength of the radiation does not change and *nonelastic*, in which the wavelength becomes lower or higher than the incident radiation. [21]

For refraction of light at the interface of two media, an important physical quantity is absolute index of refraction n = c/v, which is the ratio of the speed of light in two optical media. It plays an important role in the expression of Snell's law:

$$\frac{\sin\alpha}{\sin\beta} = \frac{n_2}{n_1} \tag{1.8}$$

where n_1 and n_2 are the indexes of refraction of the incident and transmitted media, and α and β are the angles of the incident and transmitted rays measured from the normal to the local surface. [22]

When the light ray falls on the boundary of two media with different optical properties, it changes the direction and intensity of light. The scattering of light occurs due to repetition and combination of elementary optical phenomena such as reflection, refraction and diffraction. [21, 23] Figure 1-1 shows a spherical water droplet on which impinges light ray. On the air-water interface occurs refraction of light and then light reflection inside the droplet. At the output of droplet is the light ray refracted again.

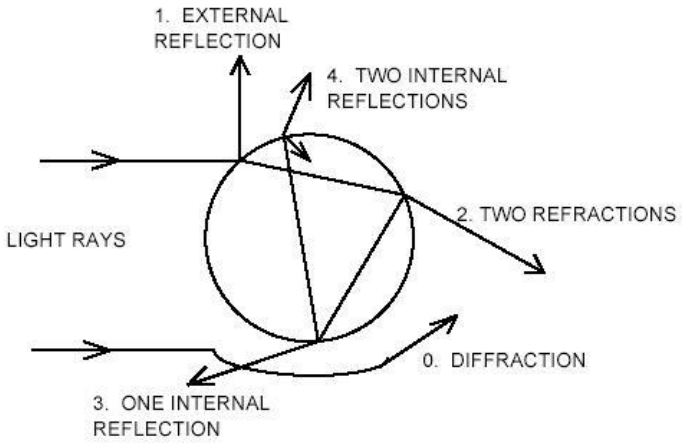

Figure 1-1 Light rays scattered by a sphere [24]

As it is mentioned in [24], the type of light scattering on particle depends on a dimensionless size parameter χ, defined as:

$$\chi = \frac{\pi \cdot D}{\lambda} \tag{1.9}$$

where D is droplet diameter and λ is the incident wavelength of radiation. Based on the value of χ, the types are:

$\chi \ll 1$– Rayleigh scattering,
$\chi \approx 1$– Mie scattering,
$\chi \gg 1$– Geometric scattering.

The first treatment of scattering was done by Rayleigh in 1871. [23] He considered the case where the particles are much smaller in diameter than the wavelength of radiation that is being scattered. This situation can be seen in Figure 1-2a.

Situations where the size of the scattering particles is comparable to the wavelength of light are known as Mie scattering (see Figure 1-2b). It is named after Gustav Mie. His theory takes into account only spherically symmetric particles, as well as surroundings from homogenous and isotropic material. According to Mie, the scattered radiation for a sphere depends only on viewing angle, index of refraction and size parameter, as discussed above. [24]

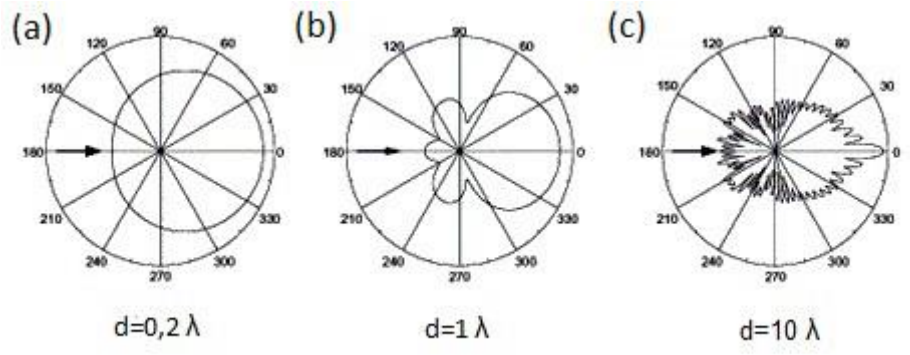

Figure 1-2 Scattering of particles with different diameters [25]

In case of $\chi \gg 1$ occurs geometric scattering (Figure 1-2c). Transmitted light of such large particle is already governed by the laws of reflection and refraction known from geometrical optics. Therefore, in this case it is usually not even spoken about scattering of light. [26]

The principle of light scattering on the spherical drop is similar for more complicated structures of the spray, such as ligaments, filaments, liquid sheets or their combination. Larger liquid structures may reflect more light and with the illumination from the front and side (in relation to the camera) they will appear brighter and with the back illumination darker. This have been observed by Sridhara and Rghunandan [27]. For the visibility of the liquid stream (which is the special case of ligament) and individual droplets can be used source of light of low power, such as conventional xenon flash light, because the liquid is discharged from the exit orifice at relatively low velocity and with the use of flash light and DSLR camera is able to capture this movement sharp. In comparison with the liquid sheet where the fluid velocity is higher a motion blur is presented and the use of the light source with shorter exposure time is needed. This provides pulsed lasers which can „freeze“ fast liquid motion and provide detailed informations about the phenomenon.

2.3 Classic visualization

The location of light refers to the interaction between used light source, object and camera. The following terminology describes the location of the light in a relation to the subject. Commonly reported lighting techniques in the field of spray diagnostics involve front lighting, side lighting, and back lighting.

2.3.1 Front lighting technique

Front lighting is probably the most common form of visualization. In this technique, the illuminating source and the camera are placed parallel (see Figure 2-3), hence the reflected light from the object is captured.

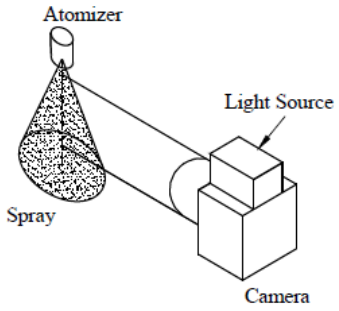

Figure 2-3 Front lighting scheme [27]

In the study of Sridhara and Raghunandan [27] was this technique applied to airblast and swirl atomizers with the use of a flash light mounted on the camera. In the case of spray from an airblast atomizer the photographs appears dull due to weak reflective signal of smaller water droplets. In the case of swirl atomizer the liquid sheet shines due to comparatively higher signal strength from the large surface area of liquid sheet. From the images of swirl atomizer are obvious shine boundaries of the object and dark inner regions, which is a result of masking of inner regions by the droplets at the outer regions. Another author in [28] applied front lighting technique in his study of the spray core characteristics. A stroboscopic light was used as a light source and the images obtained from the CCD camera were used for measuring the spray cone angle. The results showed that the spray cone angle is increasing with the increase of Reynolds number (which relates to the determination of regime changes from unstable to transitional).

From the foregoing is clear that front lighting is useful to record the external appearance of the spray, but it fails to reveal any inner details. This technique is suitable for evaluation of the spray cone angle, spray width, penetration and dispersion. The advantage is its simple setup and the light source of normal power.

2.3.2 Side lighting technique

One of the most popular side lighting technique is Planar Laser Imaging (PLI). This approach provides qualitative and quantitative two-dimensional information of spray structure. [29]

Kristensson [30] describes the principle of this technique in Figure 2-4. The incident laser beam is first expanded in one direction by a negative cylindrical lens. The beam is then collimated using a positive spherical lens, which compresses the light in the other direction, thus creating a sheet of light. In some applications, a diverging laser sheet is preferred which can be achieved by replacing the spherical lens with a cylindrical one. Regardless of which, the light is then guided through the object and the signal is recorded, usually on the CCD camera positioned at 90 degrees.

Ďurdina et al. [31] used this technique to capture the spray from the pressure swirl atomizer with kerosene as a tested liquid. From the images can be seen especially inner informations of spray such as liquid sheet breakup length, spray cone angle or creation of droplet clusters.

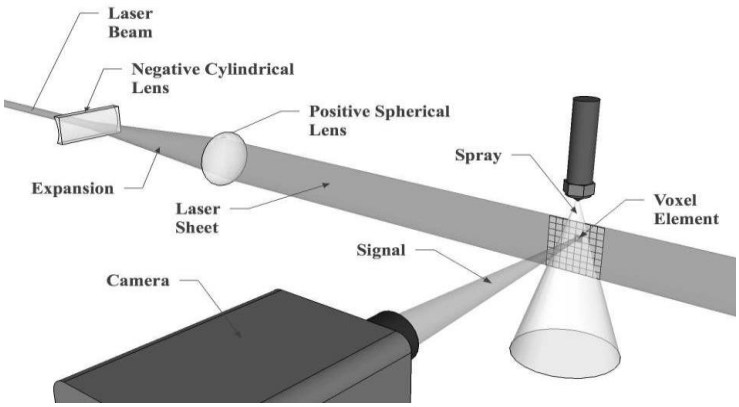

Figure 2-4 Planar laser imaging [30]

2.3.3 Back lighting technique

In the present study the term "back lighting technique" referres to the shadowgraphy technique in which the shadow of the object is recorded. This technique is frequently used for a heat transfer region, visualization of shock waves or shape of streams, spray analysis, droplet impaction/coalescence, particle size and shape, bubble formation and growth, ballistics, welding, etc. [13] More detailed information about shadowgraph method can be found in [13, 22]

According to Smits and Lim [22], the principle is to produce parallel light that is incident on the nonuniform transparent object. A schematic diagram is on Figure 2-5. The light source must be small enough, but with sufficient intensity to suffer a lack of sharpness due to diffraction. In case of using large-scale optics, a second spherical lens reduces the size of the image. The trajectories of light rays passing through the field are bending due to refraction at an angle from the original path. If the second derivative of refraction is not constant, the shadowgraph will visualize the density changes, which results in irregular surfaces with various shades. If the gradient of the refractive index is constant (the density has a linear progression), the plane of observation will appear uniformly illuminated, but with lower exposure. Consequently, the shadowgraph is useful to visualize the areas having a non-constant second derivative of the refractive index.

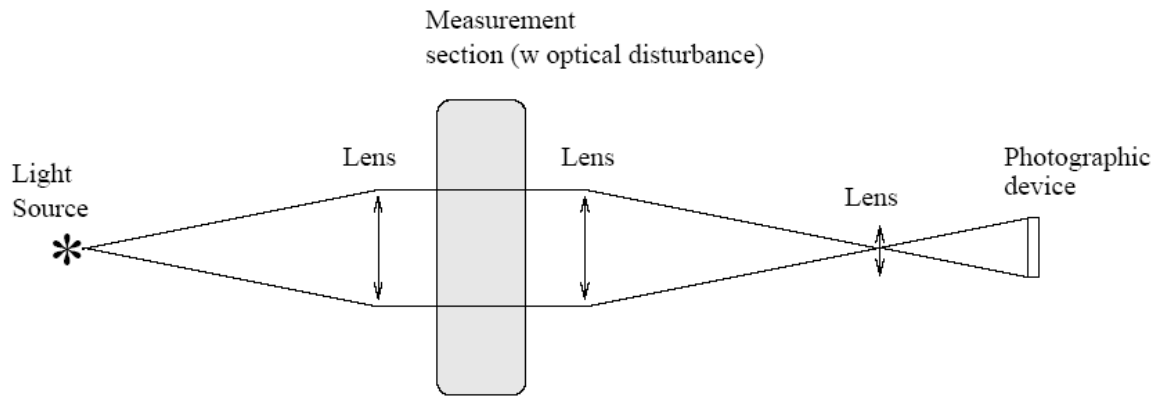

Figure 2-5 Geometric diagram of a shadowgraph system [32]

Finding quotes by Sridhara and Raghunandan [27] have revealed that there are two ways of capturing the shadowgraphy image. In the first one, the camera lens is focused to the centerline of spray, so only the liquid core at the center would appear sharp and the rest with dull boundaries. In the second one, the camera lens focuses the image on the opposite side from which the image is received into a translucent screen. This technique is not able to provide details about the internal structure of the spray in order to obtain a nonrealistic disproportional image, which shows a large images of droplets located closer to the light source and relatively smaller images of droplets that are closer to the screen.

The great advantage of shadowgraphy is its extreme simplicity, adaptability to large field-of-view and high sensitivity to the second derivative of refractive index. The disadvantage is that the shadowgrams are not in 1:1 correspondence between the object and its shadow in general. Only the dark areas can yield an undistorted perception of the observed object. If the distance of the screen is large enough, the light rays can overlap and intersect before forming resulting shadowgram. [33]

2.4 Schlieren technique

Schlieren technique is derived from the German term „die Schliere“ – local inhomogeneity in transparent media (e.g. glass). This method is being used in research of transport phenomena (heat transfer, mass transfer, transfer of momentum) where is the object of interest in the first derivation of the refractive index. [19] Another application areas includes shock physics, wind-tunnel research, thermodynamics, combustion research, flow visualization and ballistics. [33]

In schlieren system (see Figure 2-6), illumination must be produced from a point light source, which may be a mercury vapor source, spar or laser. By using a pair of mirrors or lenses, a parallel or collimated light beam is created, which passes through the flow field on to a knife edge. The diameter of the mirrors or lenses determines the image area. A knife edge is mounted on the focal plane of the second lens. [33] Smith and Lim in [22] pointed out that if there will be no inhomogeneities in the tested area, it will cause a reduction in light intensity due to the deflection of light rays. While passing through inhomogeneity, the rays are deflected which results in their displacement in the focal plane. The brightness distribution of the image corresponds a change in density, when the part of the light beam is being refracted and creating lighter or darker areas in the image.

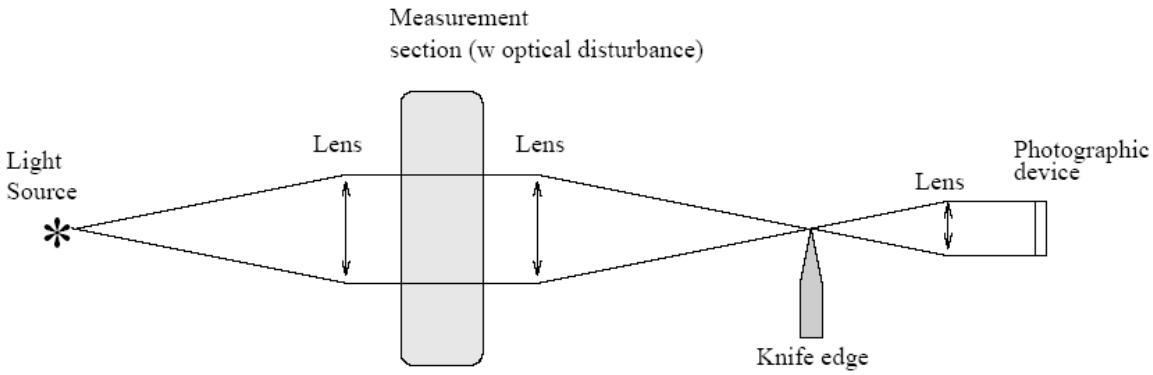

Figure 2-6 Geometric diagram of Schlieren system [32]

In comparison with the shadowgraphy, the main advantage is simple optical device and high resolution image. [26] Other benefits are high intensity measurements and imaging of the subject in real time. The disadvantage is its difficult setup and the high sensitivity to external influences (vibrations).

2.5 Holography

Holographic method captures the information on the light wave including the amplitude and phase information. According to Pavelek et al. [19], the application of the holography to spray systems is particle distribution, size and speed of particles in fluids.

The principle lays in illuminating the sample volume of moving drops with a coherent beam of light in the form of a short pulse (Figure 2-7). The measurement volume is a cylinder with diameter equal to that of the laser beam and with length equal to the total width of the spray. The duration of the laser pulse must be extremely short (20 ns), so that the droplets within the measurement volume were recorded as „frozen“. The resulting hologram captures in permanent form the location and size of a moving system of drops (drops as small as 15 μm), and then produces a stationary three-dimensional image of all the drops contained inside the sample volume. Thus, the holographic method is essentially a two-step imaging process. [2]

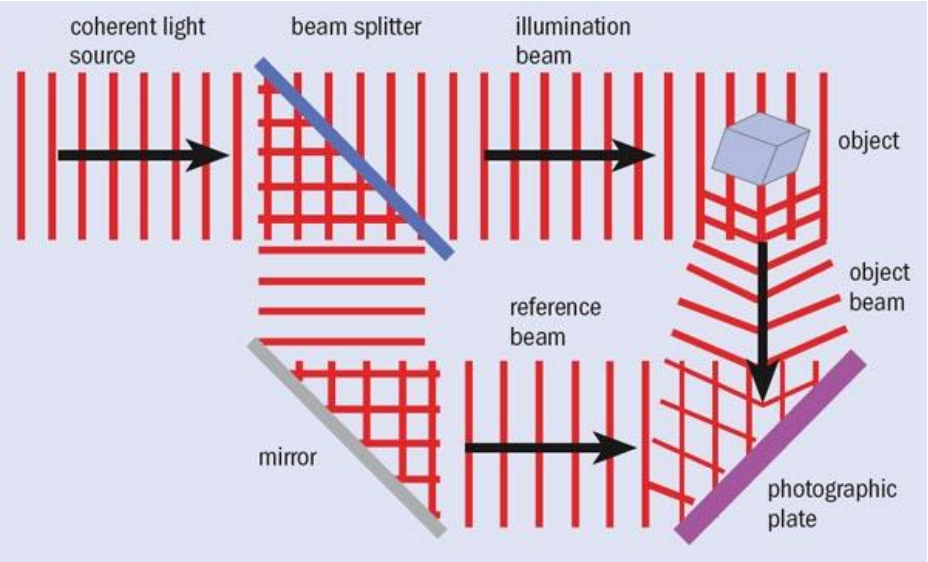

Figure 2-7 Scheme of holography [34]

For recording light wave the reference beam is used, which is brought to the photographic plate at an angle to the object beam. This appears in a finite fringe pattern as a spatial carrier frequency to record an amplitude and phase information that describes the object wave. Whereas the photographic film only responds to the irradiance, the phase information of the light wave will be lost. [22]

Lefebvre in [2] ranks among the advantages of the holographic technique recording of images that can be studied later at leisure. Another advantage lies in no calibration requirement, because the accuracy is fundamentally set by the wavelength of light. The main disadvantage is that its application is limited to dilute sprays.

2.6 Measuring techniques based on the light scattering principles

This section describes techniques which are frequently used in the examination of velocity, concentration, density and other parameters in the field of two-phase flows. More various techniques might be found in the literature, however, here I focus on just two of them which are closely related to the topic of presented thesis.

2.6.1 Particle Image Velocimetry

Particle Image Velocimetry (PIV) is a modern method of fluid flow visualization, which allows vectors measurement of the instantaneous velocity flow field. PIV has been used by many investigators, e.g. Wang et al. [35] and Feggeler et al. [36]. In a simple arrangement there are measured two velocity components in a plane. For recording all three velocity components in the space it is appropriate to use stereoscopic apparatus, as described below.

Adrian in [37] describes that the principle of PIV is based on illumination of particles, which are seeded into the flow or they naturally occur in the studied phenomena (e.g. spray droplets, aerosols, etc.). According to Ďurdina [3], the particles added into the flow have to be small enough to follow the flow without slip but large enough to sufficiently scatter light energy and form bright particle images. These particles are illuminated by a sheet of

light from pulsed laser located perpendicularly to the camera (digital/high-speed). The flow lighting and capturing of images occurs twice in a row. From the known time interval between two pulses and the measured displacement we can measure the velocity of individual or multiple particles and assign velocity vectors. The automatic analysis is possible with suitable computer advice.

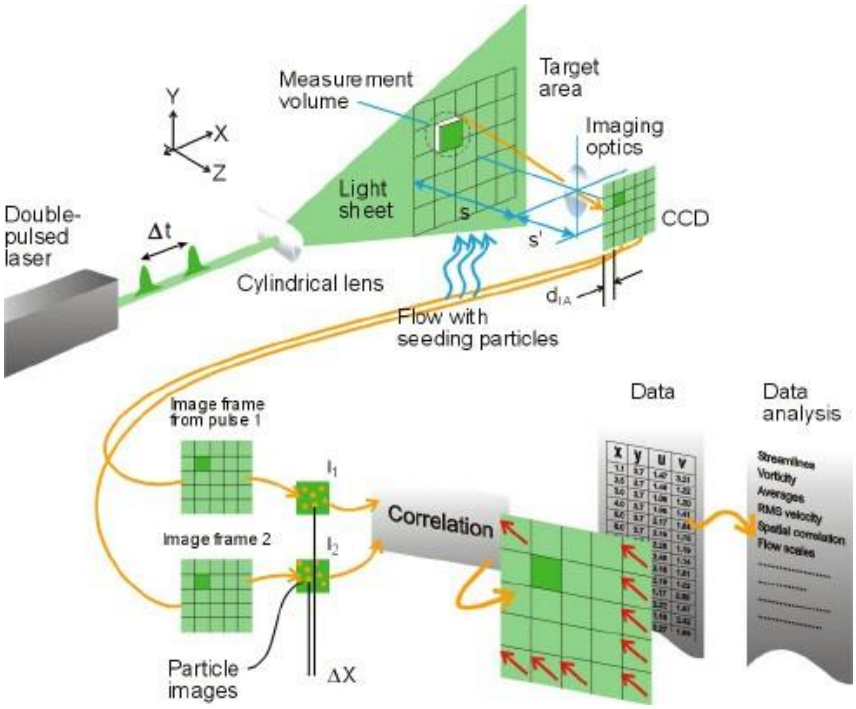

Figure 2-8 Particle image velocimetry scheme [38]

Most of the flows are three dimensional in nature, so it is essential to be able to measure all the three components to obtain the complete picture of the flow. This is enabled by the *stereo* PIV system (SPIV). This system measures three velocity components in a plane using two cameras whose optical axes form an angle of 90°. Based on the camera calibration and numerical calculations software creates a spatial vector map. [38]

2.6.2 Planar Laser Induced Fluorescence

Planar Laser Induced Fluorescence (PLIF) is nonintrusive, instantaneous flow visualization technique with high spatial and temporal resolution. From calibrated PLIF images can be derived density, concentration, temperature and velocity fields. In combination with the PIV method is possible to evaluate the mass flow in fluids. [38]

As a source of light is usually used a pulsed laser, which provide higher power than the continuous lasers. The mechanism of sheet creation is roughly the same as that for PIV (see Figure 2-8). The injected fuel is either made up of fluorescent material or seeded with a fluorescent tracer. This chemical compound is added because it absorbs the laser light energy and re-emits light at a longer wavelength that can be detected by a photodetector. [38] In quantitative data analysis should be taken into account that most tracers exhibit pressure and temperature dependencies. [39] For capturing good quality photographs it is essential to use a camera equipped with a sharp cut-off or narrow-band filter, so that only the fluorescent light is recorded. Timing is often used to synchronize pulsed light sources with camera.

Tab. 2-1 Summary of information obtainable from visualization techniques

Visualization technique	Information obtainable
Front lighting	external appearance of the spray field, spray cone angle, spray width, penetration and dispersion
Side lighting	inner sheet information, spray cone angle, liquid sheet breakup length, droplet clusters
Shadowgraphy	breakup phenomena, surface wave generation and growth, secondary atomization details
Schlieren	gradients of refractive index changes, vapors
Holography	droplet size and shape, amplitude and phase information
PIV	vector map of the velocity field, immediate and diametric images of flow
PLIF	velocity field, density, temperature, concentration, determination of scalar field

3 Equipment in visualization chain

3.1. Recording elements

Earlier, for recording of images a standard cameras with limited shutter speed were used. However, high-speed cameras and digital cameras currently dominate.

3.1.1 Digital cameras

A device that captures images behind the lens of digital camera is called image sensor. The image sensor consists of pixels that register the amount of light that falls on them. They convert the received light into a corresponding number of electrons, which are further converted into voltage and then numbers by means of an A/D converter. Subsequently, the signal produced by the numbers is processed by electronic circuits inside the camera. [40] Currently, there are two main types of image sensors used in digital cameras – CCD (Charge-coupled Device) and CMOS (Complementary Metal-oxide Semiconductor).

CCD sensor

In CCD sensor, each cell is an analog device. The light which strikes the chip is held as a small electrical charge in each photo sensor. The charges are converted to voltage one pixel at a time as they are read from the chip. The camera must be equipped with the circuitry for conversion of voltage into digital information (A/D converter). This leads to a higher consumption of electrical energy and slow data flow. CCD sensor transmits data only by lines. [41]

Advantages:

- high uniformity,
- high image quality due to a few amplifiers,
- high sensitivity,
- high dynamic.

Disadvantages:

- blooming effects,
- no direct pixel addressing. [42]

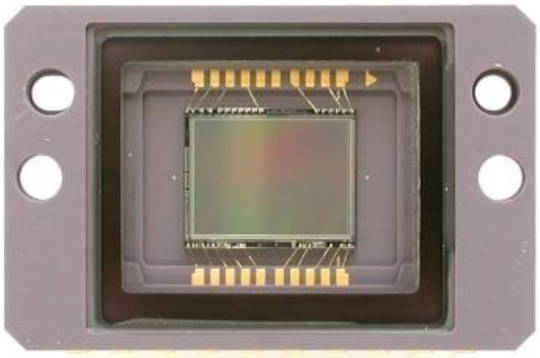

Figure 3-1 CCD sensor [42]

CMOS sensor

The CMOS sensor is a type of active pixel sensor made using the CMOS semiconductor process. Extra circuitry next to each photo sensor converts the light energy to a voltage. A/D converter on the chip may be included to convert the voltage to digital data. [42] CMOS sensors allows a higher density of elements on the chip than CCD sensors.

Advantages:

- size (implementation of devices on chip),
- A/D converter on the chip, no blooming effects,
- each pixel addressed,
- high frame rates.

Disadvantages:

- less uniformity (noise),
- lower sensitivity. [42]

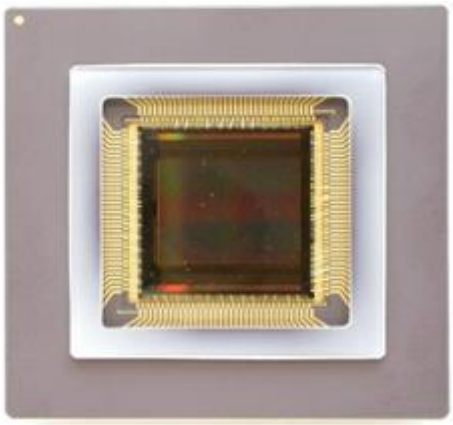

Figure 3-2 CMOS sensor [42]

3.1.2 High-speed cameras

In contrast to the digital camera described above, the high-speed camera allows recording fast-moving objects as a photographic image onto a storage medium. The high-speed cameras of today using either CCD or CMOS sensor, recording typically over thousand frames per second. There are monochrome or color film materials, but for recording and evaluating the majority of visualization experiments monochrome are sufficient. [33]

Advantages:

- a detailed time analysis and post-processing of spray,
- the images can be played back in slow-motion,
- high scanning frequency - tens of kHz in full resolution, (2,000,000 frames per second in maximum at reduced resolution),
- stability information about the spray cone development,
- the possibility of exploring dynamic phenomena.

Disadvantages:

- less power of light at the output,
- the batteries can drain out more quickly.

Figure 3-3 Photron FASTCAM SA-Z 2100K [33]

3.2 Light sources

Visual and optical experiments usually require specialized light sources. According to Smits and Lim [21], the two most common sources of lighting used in flow visualization are *conventional light sources* and *lasers*. Conventional light sources include incandescent lamps, spark gaps, compact-arc lamps, electronic flash and light-emiting diodes, and they are used to visualize external features of the flow. On the other hand, lasers are frequently used to visualize the internal structure of the flow. Moreover, it is necessary to distinguish whether the light is *continuous-wave* (CW) source, which produce radiation continuously, or *pulsed* source, which produce single or repetitive radiation pulses of short duration.

Incandescent Lamps

As it is described in [43], incandescent lamps produce light when an electric current passes through a hot filament and causes a visible light. These continuous light sources are inconvenient for short-duration use, because they are less energy efficient than other light sources. Among types of incandescent lamps are included: general bulbs, reflectorized bulbs, tungsten-halogen bulbs and xenon bulbs.

Spark gaps

Spark gaps are the oldest intermittent light sources. They consist of two conducting electrodes separated by a gap usually filled with a gas, constructed to allow an electric spark to pass between the conductors. When the voltage between the conductors exceeds the breakdown voltage of the gas within the gap, a spark forms (typically of 0.1-1 μsec duration). Their most widespread use today is in spark plugs in internal combustion engines, but they are also used in high-speed events, etc. [41, 44]

Compact-Arc Lamps

Principle of an compact-arc lamps leads in ignition a small arc between electrodes confined in a glass bulb. According to Settles [45], many arc lamps can work in either continuous or pulsed mode, with pulse durations in the microsecond range or less. A modern type of this light source is the high-pressure *mercury-arc lamp* with an arc size of about 0.2 mm and the highest luminous exitance of any light source. Thanks to its blue-green end of spectrum make these lamps excellent shadowgraph sources. On the other hand, they emit dangerous UV radiation and have some assumption of bulb explosion. *Xenon arc lamps* have a better white-light color balance than mercury arcs. Even though their luminous exitance is lower by about an order of magnitude, the dimensions of effective source are often larger.

Electronic flashtubes

Camera flashes of today are sufficient for routine capture of non-moving objects, but they cannot stop moving objects such as a bullet in flight or shock wave. They are not fast enough, because of having only a millisecond-range flash. However, this problem can be resolved by using a xenon flash as a multi-phase applications, where there is a few of separate high-speed flashes at a high repetition rate. Another, but more efficient way is the use of flash operating in the microsecond-range or faster [45].

Light-Emitting Diodes (LED)

As it is described in [45], LEDs are modern semiconductor light sources that have found application in both pulsed and continuous illumination. They are compact and cheap, but have a relatively-low light output compared to flashtubes and sparks. A typical LED has a few mW output, but 200 mW output or more is on the horizon. In compare with incandescent lamps have LEDs 10 times higher efficiency. The disadvantage is that their life highly depends on temperature.

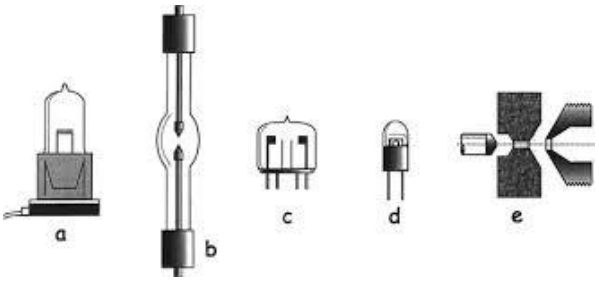

Figure 3-4 Conventional light sources: **a** tungsten-halogen lamp, **b** compact arc lamp, **c** xenon flash tube, **d** LED, **e** spark gap [45]

Lasers

A laser[1] is a device with ability to emit monochromatic, coherent and collimated light with high energy power. Each laser consists of a gain medium, a mechanism to energize it, and something to provide optical feedback. The gain medium is a material consisting of an atomic or molecular gas, solid or semiconductor material. Such material needs to be supplied with energy (electromechanical or chemical) in a process called pumping, which can be provided by a flash lamp or another laser. [41] With the use of the mirror arrangement, light oscillates within the laser material and is amplified each time. The outcoming light of the laser may form a narrow beam or be spread out. [45]

Lasers can be divided into two groups: a continuos lasers and pulsed lasers. The disadvantage of continuous lasers is relatively low power. Pulsed lasers can create a substantially higher intensity of illumination with a high frequency pulsation, therefore, preferred in applications with high flow velocities. Their disadvantage is the high cost and the need for time synchronization with camera. [26]

According to Raffel et al. [44], there are many types of lasers like Helium-neon, Argon-ion, semiconductor, ruby or Neodym-YAG laser. For more detailed information readers are referred to [44].

3.3 Optics

In many applications it is necessary to dissipate light beam or change its shape. This can be done by using optics with cylindrical or spherical lens, or their combination. Taking into account the laser beam passing through a single cylindrical lens (see Figure 3-5), the light in the output will be in the shape of a cone. If it is added the spherical lens, the cone becomes a plane.

a) single cylindrical lens b) cylindrical + spherical lenses

Figure 3-5 Conversion of laser beam into a) a light cone and b) a light sheet, adapted from [46]

[1] „Laser“ is an acronym for light amplification by stimulated emission of radiation.

4 Experimental setup

Experiments were performed on the fuel circuit in the Spray laboratory at the Brno University of Technology.

4.1 Components of the fuel line

Components of the fuel line include test bench for cold spray testing, tested atomizer and atomizing liquid.

4.1.1 Test bench

A schematic layout of the test bench is illustrated in Figure 4-1. The fuel is fed by a gear pump (3) through filters (2), flow meter (4) and control valve (7) into the atomizer (8). The fuel from the atomizer falls into a collection chamber and then it is returned by gravity to the main supply tank (1). Temperature (6) and pressure sensors (5) are also present in the feeding line. The quantity of fuel is regulated by a bypass needle valve (9). Vapors from the collection chamber are exhausting by a fan into the central ventilation.

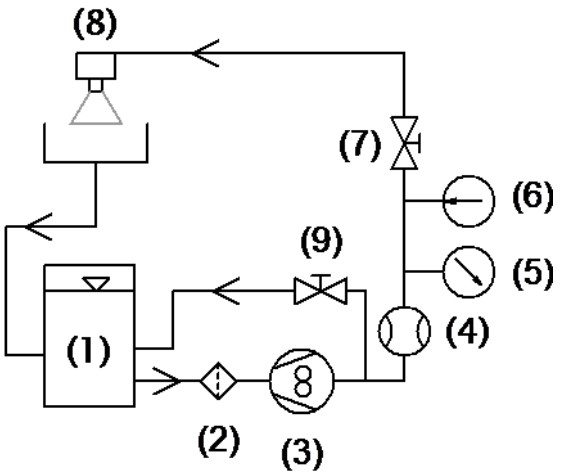

Figure 4-1 Fuel circuit with control and measuring items [47]

Measuring tools:

- Mass flow meter: Siemens Mass 2100 Di3 Coriolis fitted with a Mass 6000 transmitter,
- Pressure sensor: BD Senzor DMP 33li,
- Temperature sensor: Omega PR-13.

4.1.2 Tested atomizer

A small pressure-swirl (PS) atomizer was used for this study. Schematic layout of the atomizer and its geometric configurations are shown in Figure 4-2. Fuel is fed into the swirl chamber through three tangential entry ports having a rectangular cross-section. The atomizer air core (or spill line) was closed for all presented experiments. The PS atomizer is mounted on a three-axis traverse system for precise positioning in the horizontal as well as the vertical planes.

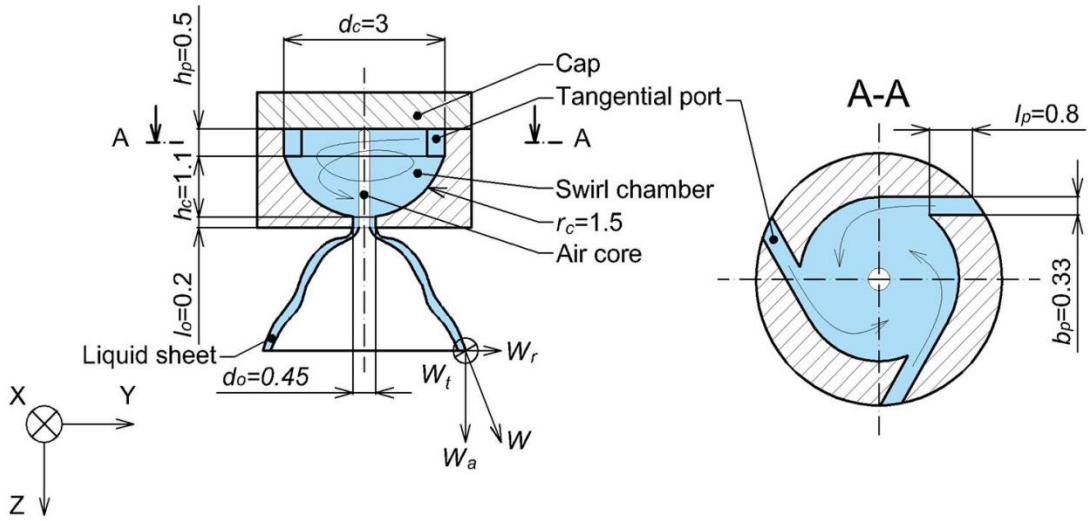

Figure 4-2 Illustration of tested atomizer

Tab. 4-1 Atomizer dimensions

Nomenclature	Description
$\mathbf{b_p}$	Width of the inlet tangential port
$\mathbf{d_c}$	Width/diameter of the swirl chamber
$\mathbf{d_o}$	Diameter of the exit orifice
$\mathbf{d_s}$	Diameter of the spill-line orifice
$\mathbf{h_c}$	Height of the swirl chamber
$\mathbf{h_p}$	Height of the inlet tangential port
$\mathbf{l_o}$	Length of the exit orifice
$\mathbf{l_p}$	Length of the inlet tangential port
$\mathbf{r_c}$	Radius of the swirl chamber

4.1.3 Atomizing liquid

Kerosine Jet A-1 was the liquid used for these experiments. Its physical properties are shown in Tab. 4-2. All experiments were done at room temperature (20 °C) and fuel was injected at three values of inlet pressure: Δp = 0.5, 1.0 and 1.5 MPa, which was set manually via gear pump.

Tab. 4-2 Physical properties of kerosene

Density [kg/m^3]	795
Dynamic viscosity [mPa·s]	1.9
Surface tension [Mn/m]	31

4.2 Components of the visualization chain

Components of the visualization chain include laser, LED panel, flash light and camera.

4.2.1 Laser

The spray was illuminated by Nd:YAG NewWave Research Gemini laser (see Figure 4-3). The laser produces 250 mJ of energy at 532 nm and operates at a maximum repetition rate of 15 Hz. This pulsed laser contains two independent laser heads mounted on a single baseplate. Both laser beams are collimated through several mirrors in one identical plane with beam diameter of 3 mm. The laser enables three trigger controls: single-shot, fixed and VAR.

For present work was used only one laser head with pulse duration of 5 ns and pulse energy of 5 mJ. During the photoshoot trigger was controlled as a single-shot.

Figure 4-3 Mobile PIV laser stand [4]

4.2.2 LED panel

Another light source used was LED panel. The LED produces 100 W of light energy. It is mounted on small three axis traverse system which enables a precise manipulation and positioning with the minimal step of 0.05 mm.

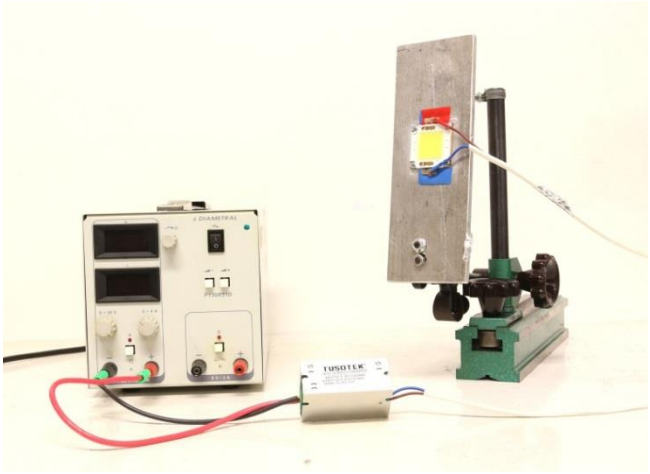

Figure 4-4 LED panel

4.2.3 Flash light

As a high-output flash light automatically compatible with the Canon camera was used the Canon Speedlite 580EX II. The flash was controlled by a wireless Canon Speedlite Transmitter ST-E2.

Figure 4-5 Flash light (right) and transmitter (left) [48]

4.2.4 Camera

Spray images were taken using a Canon EOS 70D fitted with a Canon EF 100 mm f/2.8 USM Macro lens mounted on a 68 mm long extension tube. This CCD camera allows to set an exposure time *t*, aperture *F* and sensitivity *ISO*. The camera was set up in the manual regime, because of the need to change these factors independently. With the use of WIFI service camera was remotely connected to a personal smartphone making it easier for all the handling of adjusting factors of the camera, remote shooting, or subjective observations of the images. Photo of the camera is in Figure 4-6.

Figure 4-6 Canon EOS 70D [49]

4.3 The assembly of visualization chain

Visualization chain was assembled first for shadowgraphy, then for side lighting technique.

4.3.1 Assembly of shadowgraphy

In the shadowgraph technique the light source synchronized (by hand) with the camera shutter was placed behind a translucent glass sheet and camera aperture was directly exposed to the illuminated spray (Figure 4-7). A spherical lens was used to expand the beam and the translucent ground glass sheet diffused the light to a wider region thus providing an uniform illumination of spray over the entire cross section. For flash light, LED panel and ambient light the setup was the same, but without the use of lens and diffuser.

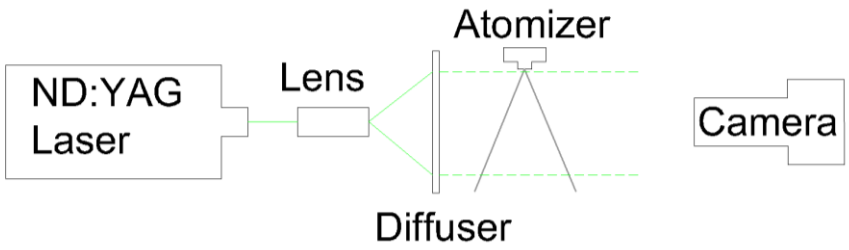

Figure 4-7 Scheme of the shadowgraph imaging system

4.3.2 Assembly of side lighting technique

In the side lighting technique, the light source was placed at the spray centerline perpendicular to the camera. Illumination by laser was carried out in two ways. In the first one, laser beam passes through the spherical lens which expand the beam to the shape of spatial cone (as in the shadowgraphy). For this case of illumination term „*laser cone*“ will be used. In the second one, directly on the laser both cylindrical and spherical lenses are mounted immediately forming laser plane with thickness of 3 mm (see Figure 4-8). For this case of illumination term „*laser sheet*“ will be used. In case of flash light and LED panel no optical elements were not needed.

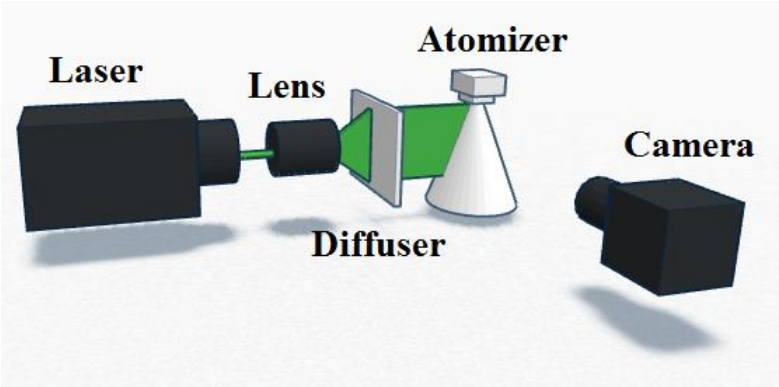

Figure 4-8 Scheme of the side lighting technique, illumination by laser sheet

4.4 Optimization of the visualization chain settings

To capture high-quality images it is necessary to know the effects of the individual components of the visualization chain on the resulting image. These effects can be detected by changing the adjustable factors for individual components and their appropriate combination.

Effect of the camera

For the camera it is need to understand three things – the aperture, the shutter speed, and the ISO.

The aperture controls light that passes through the camera lens. The smaller the aperture, the greater the opening and the camera sensor thus receives more amount of light. The aperture sizes are measured by f-stops. A higher f-stop means a smaller aperture hole while a lower f-stop means a bigger aperture opening.

The shutter speed is the duration of time a camera shutter is open to allow light into the camera sensor. Shutter speeds are usually measured in fractions of a second. Fast shutter speeds allow less light into the camera sensor and are used for high-light and daytime photography while slow shutter speeds allow more light into the camera sensor. It is obvious, that slow shutter speeds are ideal for nighttime photography.

ISO is all about the sensitivity level of the camera to available light. Usually, it is measured by numbers. A lower number represents lower sensitivity to light while higher number mean heightened sensitivity. The drawback in using increased sensitivity is that it produces noisier images, which can greatly affect the quality and subsequent evaluation. Simply put, you end up with grainy pictures if you use high ISO. For this reason it is a primary effort to maintain the value of the ISO minimum possible.

Effect of the laser

The influence of this component on the output can be detected by changing the laser power or the width of light plane. The laser power can be varied between values of 0.01–2 W. Optimum value of the power was at this stage of the research experimentally determined in accordance with best practices. The geometry of the plane can be changed by replacing of the spherical lens with cylindrical.

4.5 Image processing

Processing of each image included a subtraction of background, intensity thresholding and color correction. The evaluation of captured images was carried out in Photoshop – which deals with background subtraction and intensity thresholding, PCO Picture – which adjusted colors and created mean and RMS images, and IrfanView – which measured droplet sizes or breakup distance.

4.5.1 Background subtraction

In raw images often occur unwanted background signals such as reflections and room light, inhomogeneous distribution of light or dust particles. For all experimental runs, corresponding background images were created (image without the spray) and subtracted from the spray images. This procedure effectively reduces image noise.

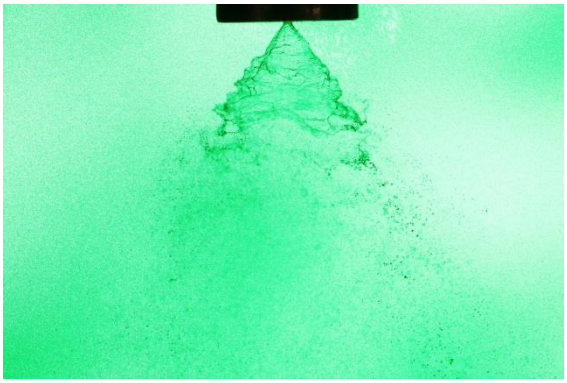

Figure 4-9 Original image, 0.5 MPa

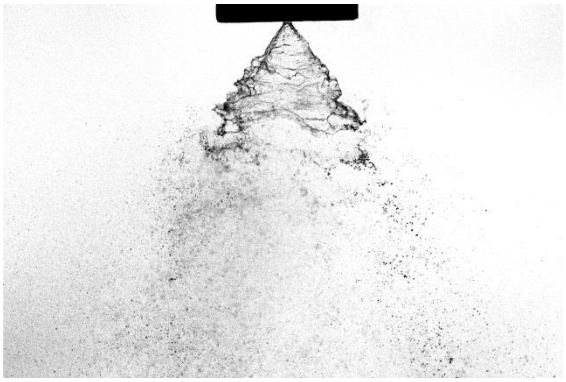

Figure 4-10 Background subtraction, 0.5 MPa

4.5.2 Intensity threshold

The next important step is to choose the correct threshold intensity of light that will be visible on the image. There are no „natural thresholds“, so this is a matter of subjective assessment. During this process it is essential not to lose (or add) any significant information from the image.

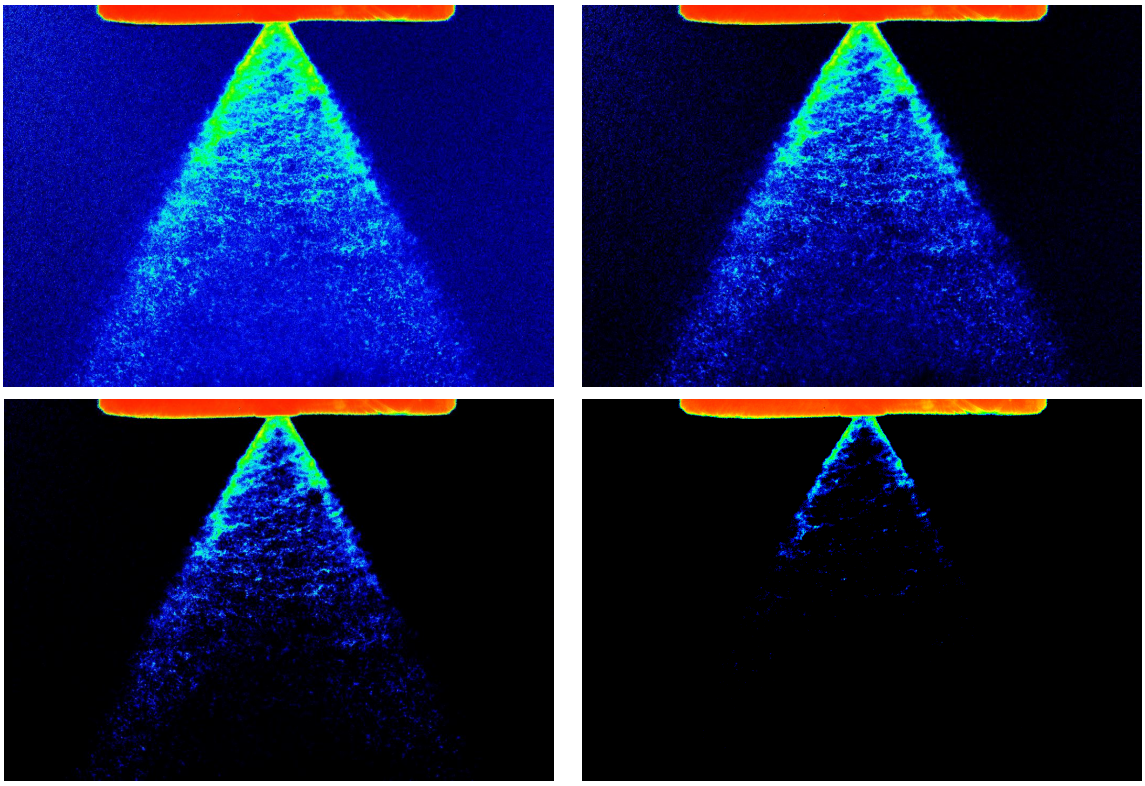

Figure 4-11 Example of the intensity level thresholding, mean image, 1.5 MPa

4.5.3 Color scales

The human eye can not distinguish shades of gray as well as the color spectrum. Therefore, it is preferable to display images with the use of colors, see Figure 4-12.

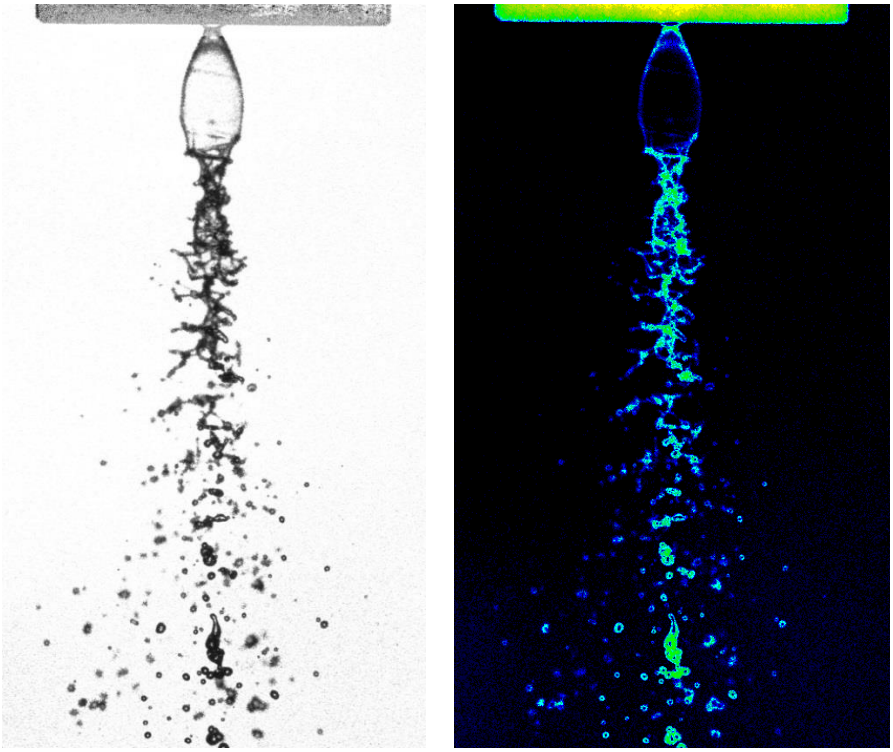

Figure 4-12 Comparison of the spray in shades of gray and colors, low pressure

5 Results

In this chapter, experimental results of the spray generated by the pressure-swirl atomizer are presented and discussed. Firstly, I tried to find the best light source for visualization of sprays. Secondly, I tried to define how to illuminate several cases of flow (such as spray, liquid stream, or the Scrubber), where I used previously gained experiences.

5.1 Influence of the light source and its location

This part of experiment discusses the influence of used light source and its location in the visualization chain on the final image quality. From the available light sources were used LED panel, flash light, laser and the ambient light in the laboratory. Each mentioned source of light was first used in shadowgraphy and then in side lighting technique. The images were captured 25 mm from the exit orifice at inlet pressure of 1.0 MPa.

5.1.1 Shadowgraphy

The liquid emerges from the atomizer at relatively high velocity and disintegrates in a close distance from the exit orifice in the form of a well-defined hollow-cone spray. To capture a sharp and detailed image will therefore need very fast shutter.

Figure 5-1 shows four types of the light sources used for this experiment. The first spray images were captured using ambient light in the laboratory, which is a special case of shadowgraphy. But a very long exposure time (2 s) caused a motion blur over whole image, which gave no information about the spray structure. Slightly better is LED light which indicates on an edge of the liquid film. But the spray is still fuzzy, even at very fast shutter speed (1/8000). With the use of flash light with exposure time about 50 μs was partially captured the structure of the liquid, but still blurry. The last option of light sources was pulsed laser which transmits a very short pulse length of 5 ns (equivalent of shutter speed $1/20 \cdot 10^6$) at which the spray appears as „frozen“. Thus captured image provides detailed information about the breakup distance, process of atomization and it points on the spray instabilities. Using pulsed laser proved to be the best way of spray illumination.

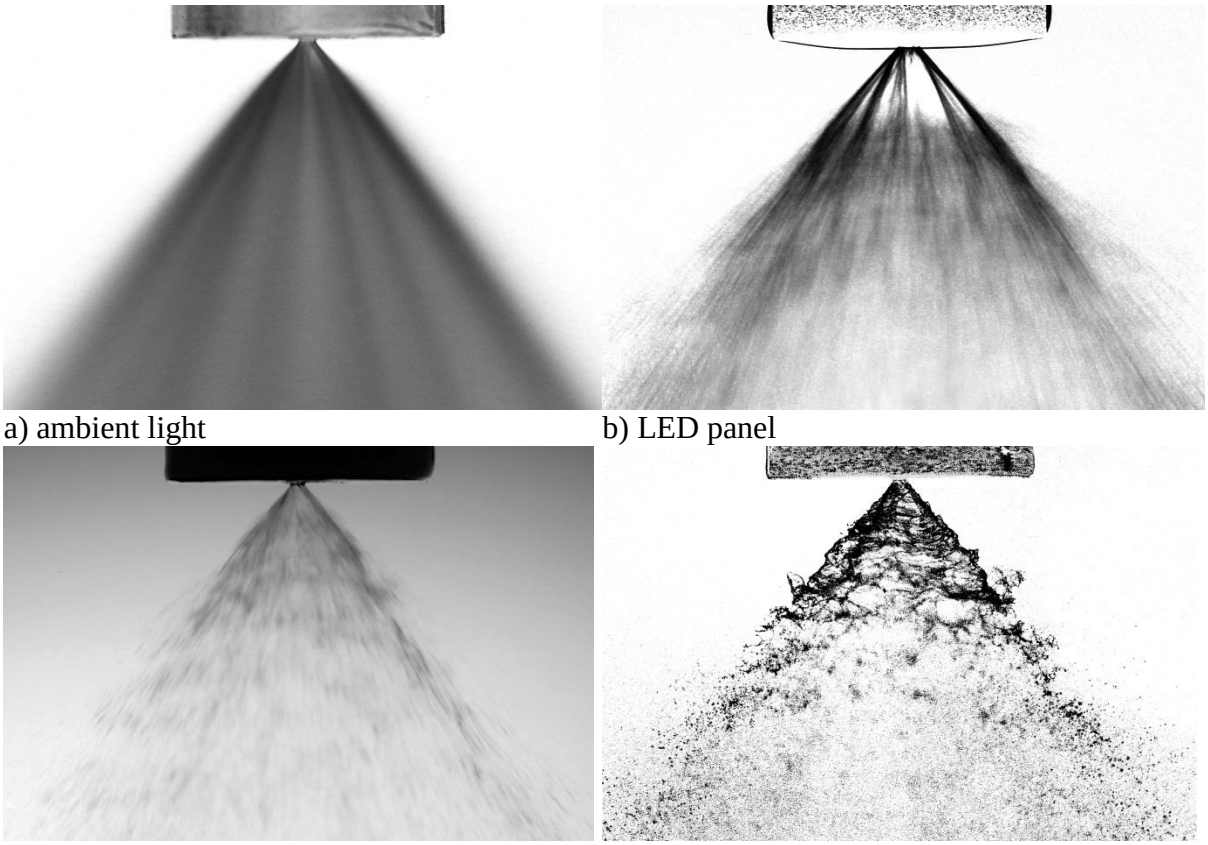

a) ambient light b) LED panel

c) flash light d) laser cone

Figure 5-1 Comparison of four types of light sources for shadowgraphy, 1 MPa

5.1.2 Side lighting technique

The technique of side lighting should provide information about the internal structure of the spray. As in the case of shadowgraphy, LED and flash produces a blurry image, because the exposure times were too long. Illumination with the laser cone clearly shows the area of the primary atomization, but still nothing more. However, Figure 5-2d) indicates the illumination with laser sheet, which can „cut“ the spray in the middle. It is evident that the spray core is formed mainly by smaller drops and at the spray periphery droplet size increases. Further downstream in the spray core droplet clusters are presented, which can be seen much better in Figure 5-3 (taken from distance of 50 mm). Such clusters are the results of the interaction between spray and ambient air. Illumination with laser sheet has proved to be the most effective way from the other compared.

a) LED panel

b) flash light

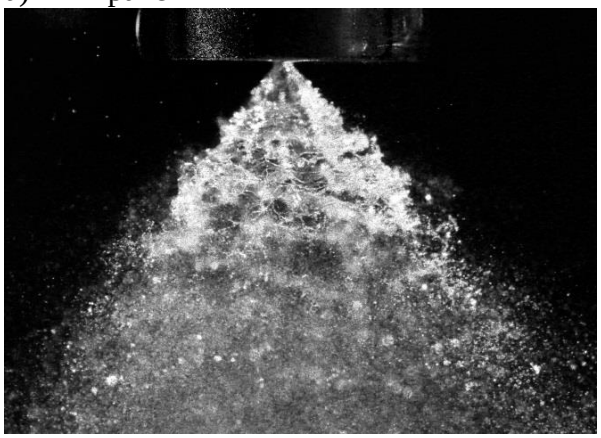

c) laser cone

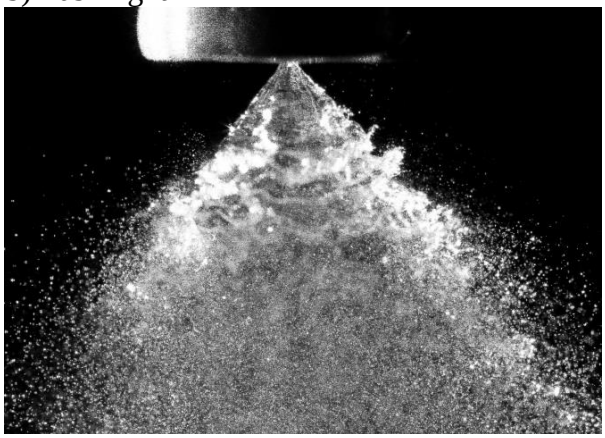

d) laser sheet

Figure 5-2 Comparison of four types of light sources for side lighting technique, 1 MPa

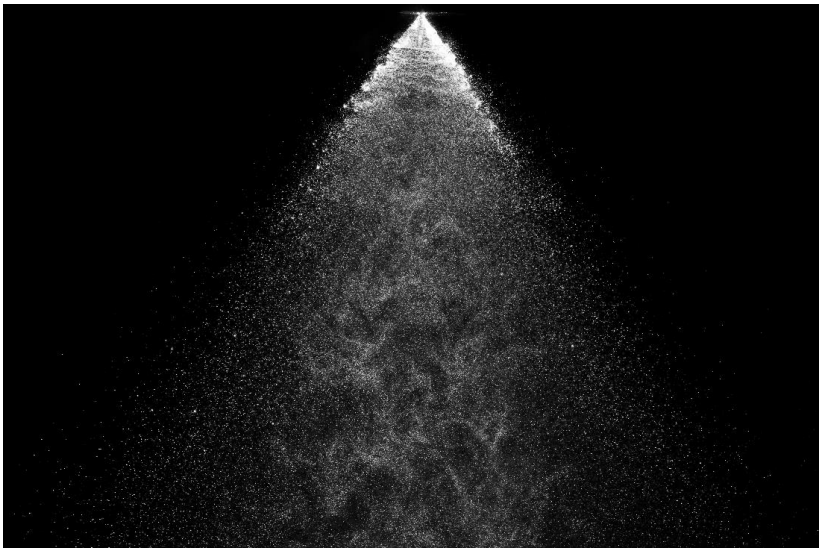

Figure 5-3 Example of droplet clusters, 50 mm

5.1.3 Liquid stream

The influence of the light source can be easily observed also on the images of liquid stream, see Figure 5-4. From the images captured by shadowgraphy the laser provides the best results. However, in the case of side lighting a very good result was achieved using the

flash light due to relatively low velocity of discharged liquid. It is an advantage for this purposes because the laser light is too expensive. For complete assessment of liquid disintegration process a combination of shadowgraphy, side liqhting (and sometimes front lighting) is suitable.

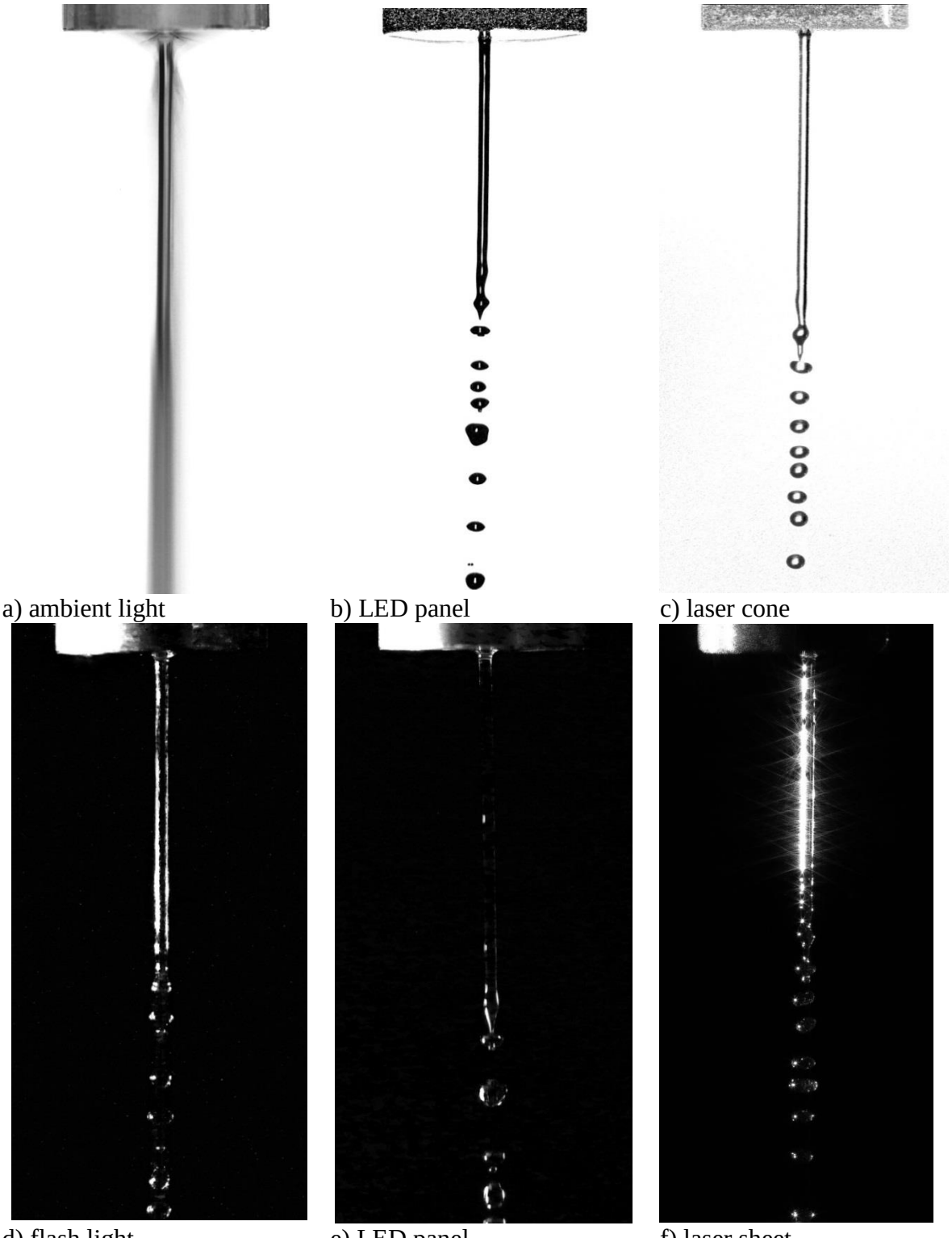

a) ambient light b) LED panel c) laser cone

d) flash light e) LED panel f) laser sheet

Figure 5-4 Comparison of the liquid stream illumination – shadowgraphy (top), side lighting technique (below)

5.2 Spray cone angle

The spray cone angle (SCA) is an important characteristic of a PS atomizer. Sufficiently large spray angle ensures better dispersion of the fuel drops throughout the combustion volume. This has an impact on ignition performance, flame blowout limits and the pollutant emissions. [2] According to Chen and Lefebvre [50], SCA depends on the atomizer dimensions and liquid properties.

Evaluation of the SCA from the photographs have to be carried out in close distance from the exit orifice, see Figure 5-5. Here, the angle of spray can be described as green and red zone on spray boundaries.

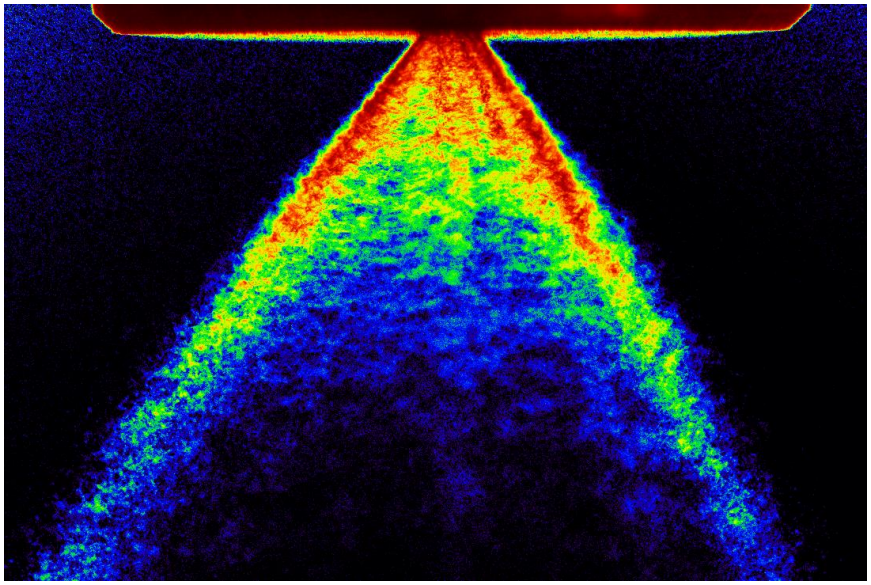

Figure 5-5 Mean image from 11 photographs, 1 MPa

5.2.1 Spray instabilities

In the area of primary atomization the stable atomizer produces well-defined liquid wall which further disintegrates into filaments and then droplets. The unstable atomizer practically do not form a continuous liquid wall, but it depends on in which part of the pulsation the image was created. From the photographs in Figure 5-6 it is obvious that the SCA significantly rises if the spray pulses. Instabilities result in the production of large droplets, which is undesirable phenomenon, it can also affect the weight distribution.

The degree of fluctuations at a given point should be determined based on the root mean square (RMS) images, see Figure 5-7. Green color corresponds to the high value of the RMS. Near the atomizer the spray is dark because there is a consistent liquid. Although in these areas may exhibit instability, liquid blocks the passage of light, thus the information is partially hidden. However, for a global assessment it is negligible, the most important are the edges of the spray that enable relevant information (in Figure 5-7 this limit is marked with red boundaries). At the spray core information are distorted because we are looking at the conical surface and the 3D aspect of the problem would have to take into account. From the images can be directly determine the degree of the SCA pulsations.

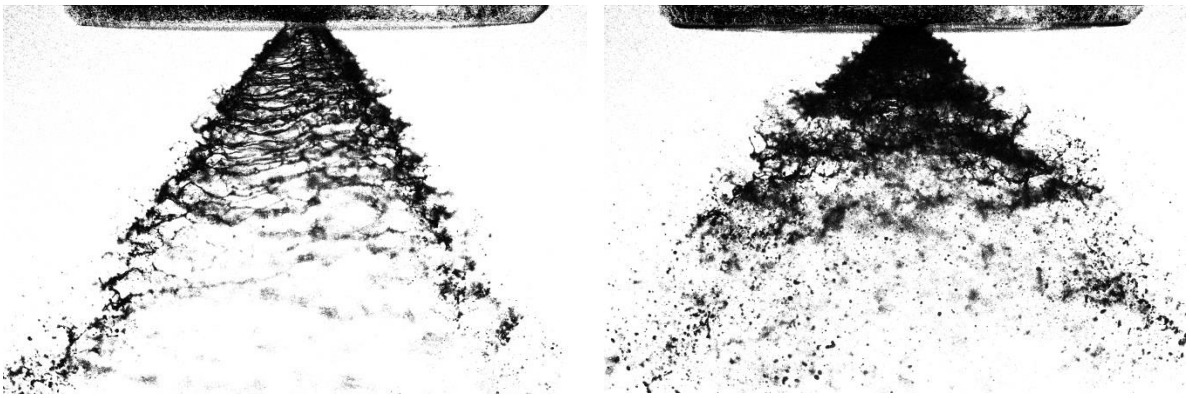

a) stable spray b) pulsating spray

Figure 5-6 Example of the stable and pulsating spray at 1 MPa

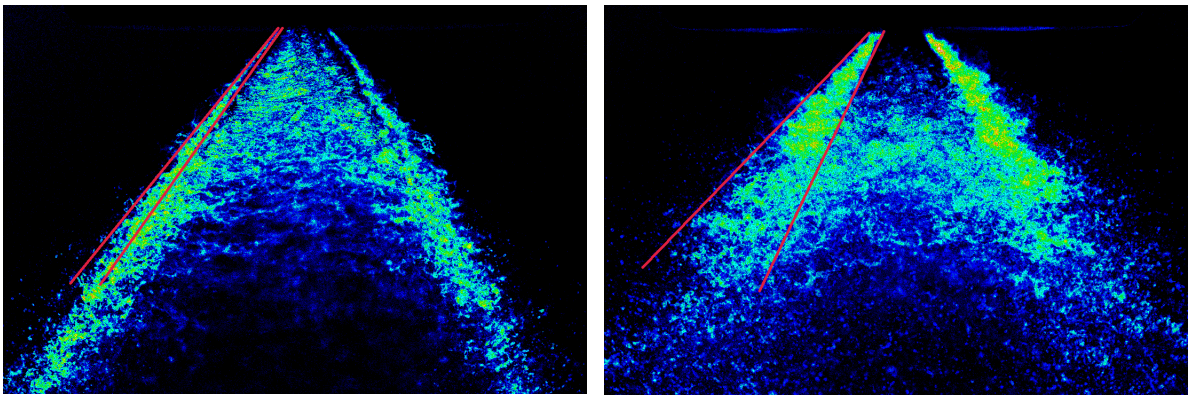

a) stable spray b) pulsating spray

Figure 5-7 RMS images of steady and pulsating sprays from 11 photographs

5.2.2 Influence of the liquid injection pressure

The SCA highly depends on the injection pressure of the liquid. (Figure 5-8). At very low inlet pressure liquid emerges from the atomizer orifice in the form of a *distorted pencil*. The detaile of breakup of this case has been described in section 1.4.2. With increasing pressure is first formed a closed bubble due to surface tension forces, and after their overcoming hollow bubble starts to develop. This stage is called an *onion stage*, according to Lefebvre [2]. A further increase in pressure leads to breaking of the lower part of the bubble which disintegrates into drops. The rest of the hollow bubble is expanding and forms a *tulip shape*. From this moment the liquid sheet may be considered as fully developed. With higher pressure the SCA gradually straightens and extends, the thickness of liquid sheet is reduced and thus the breakup distance.

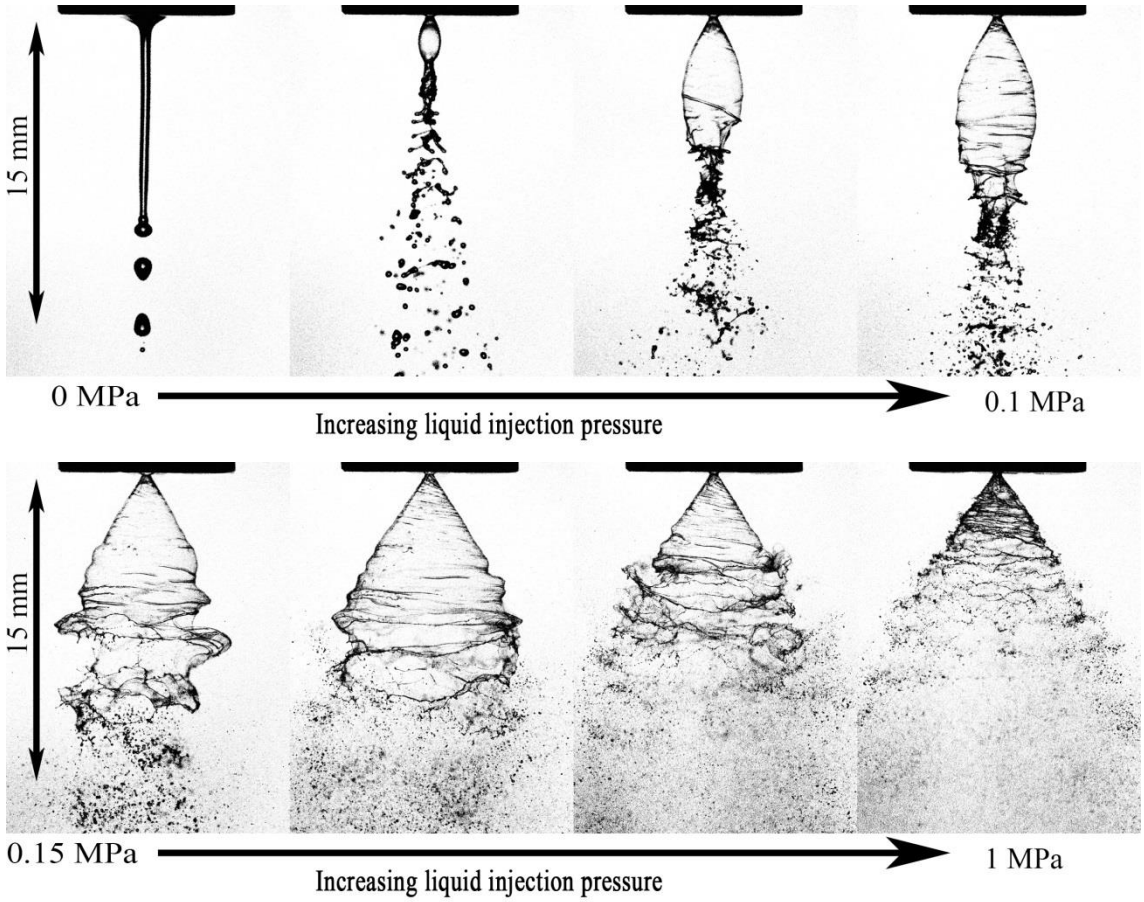

Figure 5-8 Development of spray as a function of liquid injection pressure

The images describe only the outer boundaries of the spray and provide no information on symmetry of liquid within the spray. For this reason is therefore possible to give priority to the measurement of so-called *effective* SCA [50]. For assessment of non-uniformities of the spray is suitable to use e.g. mechanical patternator, however it is no longer a matter of visualization.

5.3 The Scrubber

The results from this part were presented in the private report for a customer, who wanted to solve the possibilities for research and basic spray analysis from a pressure spiral atomizer as used in a, so called, Scrubber device.

The spiral atomizer formed three concentric hollow cone sprays (with a maximum cone angle of 170°) which are protected by a plexiglass container. Experiments were performed at room temperature (20 °C) with drinking water supplied at an inlet pressure of 0.09 MPa and a flow rate of 3000 l/h. Higher pressures were not possible due to an undersized pump.

For the assessment of the spray morphology a modified version of classic photography was used due to limited optical access to the spray. The modification was in the illumination direction as it was not possible to use direct backlighting due to reflections from the walls of the plexiglass container. For this reason, the photographs were acquired at different distances from the spray perpendicular to the first liquid wall with indirect lighting by pulsed laser. However, this method is still able to detect the liquid breakup length, as well

as primary and secondary breakup zones. It also allowed estimates of drop sizes to be made.

The liquid sheet breakup process is shown in Figure 5-9. Direct from the nozzle a continuous liquid sheet is generated, which maintains its integrity for up to 30 mm downstream. After approximately 60 mm downstream the sheet shows perforations occurring. Following a relatively short primary breakup region (Figure 5-10), ligaments arise from the liquid sheet that almost immediately form individual drops, i.e. within the secondary breakup region. Further downstream, 100 mm from the nozzle, the droplet size and structure does not change.

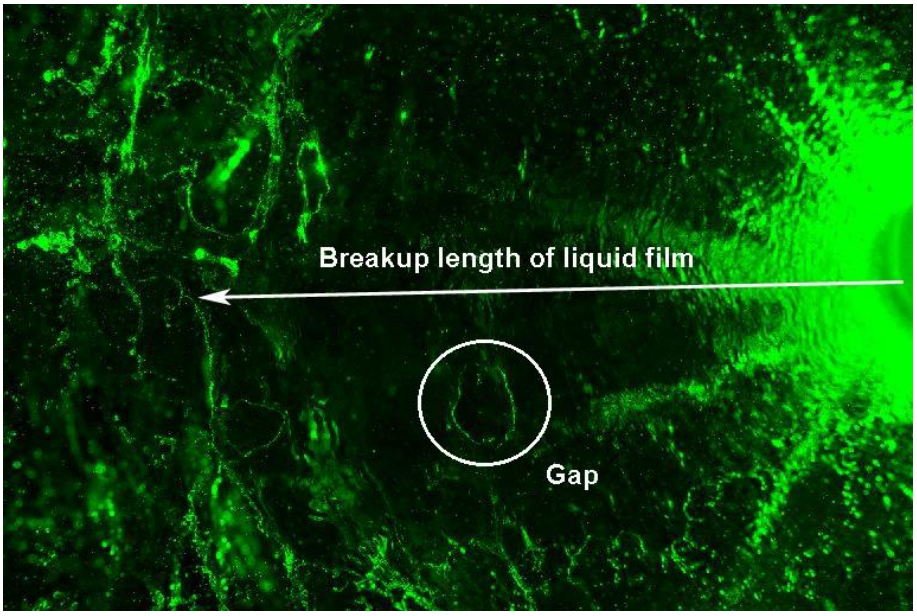

Figure 5-9 The process of liquid wall breakup

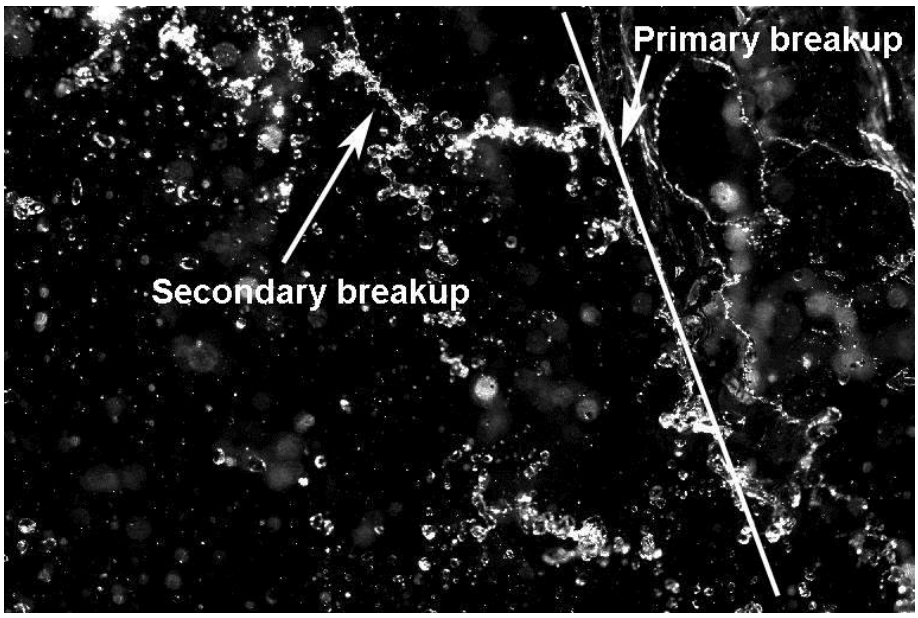

Figure 5-10 Detail of primary and secondary breakup

Measurement of droplets

Furthermore, the sizes of droplets in the spray were measured. Unambiguous recognition of a droplet was taken as a clearly defined in focus object. This spray contains both near spherical, ellipsoidal or irregular droplets. Figure 5-11 shows typical examples of droplets evaluated.

For the nonspherical droplets two diameters were estimated – indicating the major and minor axes and then the arithmetic mean was calculated, see Figure 5-12.

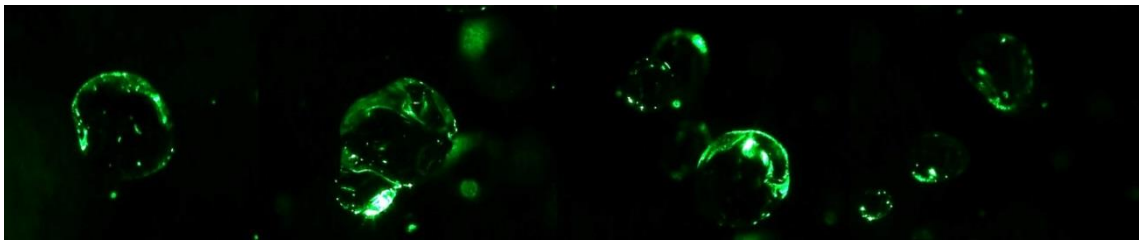

Figure 5-11 Evaluated drops, original picture

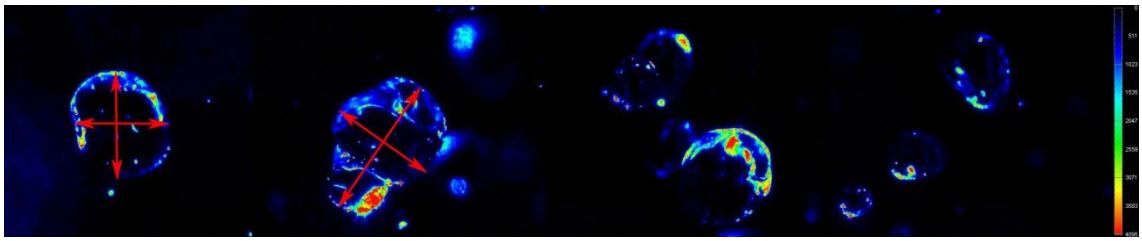

Figure 5-12 Photo finish and measured averages

From a sample of 60 drops the average droplet size to 2.5 mm was determined. Their size distribution corresponds to Figure 5-13. Droplets less than 1 mm were not evaluated because it was not possible notice them on the image. Moreover they also contained a very small liquid mass flow when the droplet diameter such as 0.5 mm has a volume 64 times smaller than a drop with a diameter of 2 mm. Most droplets are located in size class of 1-3 mm.

Other representative characteristics were determined by the percentage of the surface, resp. fluid volume (Figure 5-14, resp. Figure 5-15) in the individual size classes. From these characteristics is evident the influence of large droplets, the largest surface area and volume have size class of 2-3 mm. Simultaneously the largest drops have impact, e.g. 3 % of the largest droplets of the total (one each in class 6-7 mm and 7-8 mm), which containing 42 % of the total volume, but only 21 % of the total surface.

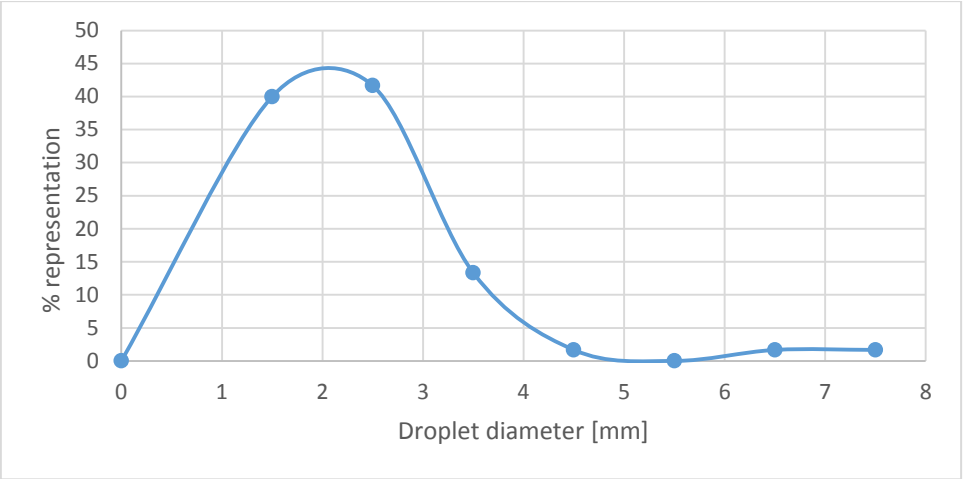

Figure 5-13 Droplet size distribution

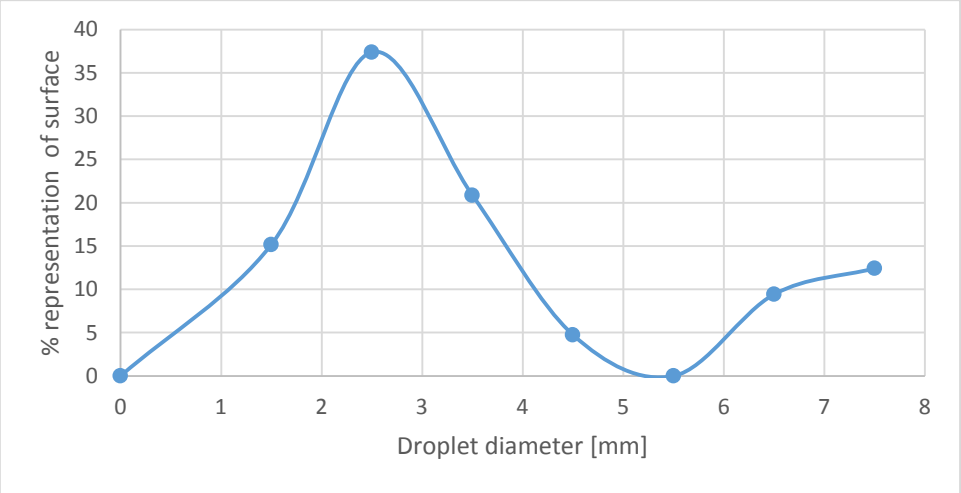

Figure 5-14 Proportion of droplets surface in individual size classes

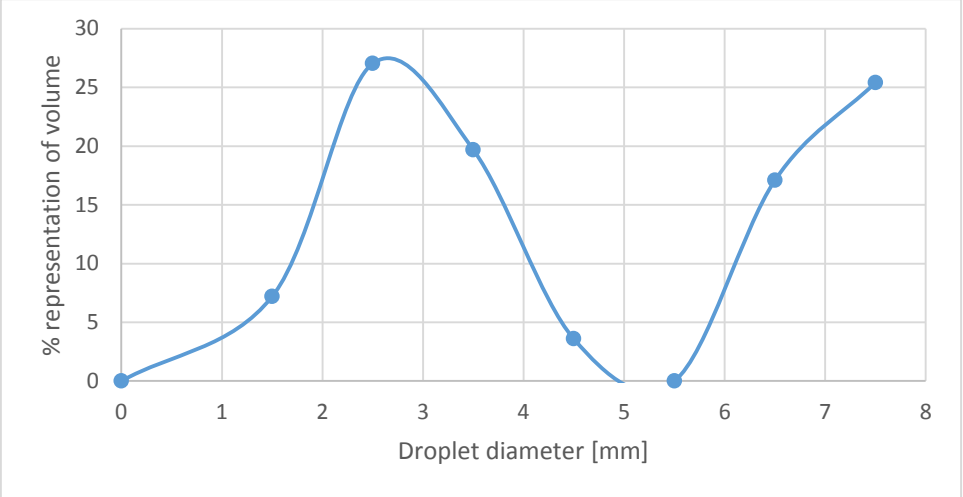

Figure 5-15 Proportion of droplets volume in individual size classes

6 Conclusion

The theoretical part describes, in detail, the processes of liquid atomization, visualization techniques for its capturing and the analysis of elements in the visualization chain. Following experimental part contains a compilation of visualization techniques, optimization of the individual elements and the image post-processing. Furthermore, a series of experiments was discussed and analyzed.

For the initial documentation of the spray formed by pressure-swirl atomizer, shadowgraphy and side lighting technique were chosen. For each method several types of light sources were tested, such as flash light, LED panel, pulsed laser and ambient light in the laboratory. Their effect on the image quality was primary investigated. It was found that both visualization techniques achieve the best results with illumination by pulsed laser. In case of shadowgraphy, using the laser enable to monitor in detail the process of atomization, the breakup distance, spray cone angle, droplet size or watch spray instabilities. In case of side lighting by laser sheet the spray is „cut“ in the middle, which provides information on the distribution of droplet size in the spray or formation of droplet clusters in the spray core as a result of the interaction between liquid and ambient air.

There are also presented images taken primarily by shadowgraphy to verify the suitability of this method. The influence of inlet pressure and spray pulsations to spray cone angle was observed. The results showed that increasing inlet pressure leads to a rapid increase of the spray cone angle. Instabilities also increase the spray cone angle, since the spray breakup is not continuous but periodic, which is influenced by wrong design of atomizer.

The last part of results is dedicated to documentation of the pressure spiral atomizer used in the Scrubber device supplied by a customer. Information gained from the previous chapters were applied and used to describe the atomization process at the atomizer. Here, a specially adapted shadowgraph technique captured and measured region of primary and secondary atomization, breakup length of liquid sheet and the size distribution of droplets in the spray.

Bibliography

[1] Lefebvre, A. H., 1998, "Gas turbine combustion", 2nd ed. Taylor & Francis, Boca Raton. ISBN 1-56032-673-5.

[2] Lefebvre, A. H., 1988, "Atomization and sprays", Hemisphere Pub. Corp., New York. ISBN 0-89116- 603-3.

[3] Ďurdina, L., 2012, "Measurement of spray characteristics using optical measurement methods", Master thesis, Brno University of Technology, Brno.

[4] Zaremba, M., 2013, "Influence of operational conditions on spray characteristic of twin-fluid atomizers", Master thesis, Brno University of Technology, Brno.

[5] Malý, M., 2014, "Quality of fuel atomization from small pressure-swirl atomizers", Bachelor's thesis, Brno University of Technology, Brno.

[6] "Corrosionpedia". [Online], https://www.corrosionpedia.com.

[7] Nakayama, Y., and Boucher, R., 1998, "Introduction to Fluid Mechanics". Butterworth-Heinemann.

[8] Pimentel, R. G., 2006, "Measurement and prediction of droplet size distribution in sprays". Quebec: Université Laval.

[9] Nabah, B. A. J., 2003, "Swirl orientation effect on the instability and the breakup of annular liquid sheets". Ph.D. Thesis. University of Cincinnati.

[10] Rayleigh, L., and Strutt, J., 1878, "On the instability of jets". Proc. London Math. Soc., Vol. 10, pp. 4-13.

[11] Weber, C., 1931, "On the disruption of liquid jets". Math. Mech. 2.

[12] Agraval, K. S., 2013, "Breakup of Liquid Jets". ISTREAMCAS, India: Vadodara, pp. 487-496.

[13] Altieri, A., Acharya, L., and Cryer, S. A., 2014, "Mechanisms, experiment, and theory of liquid sheet breakup and drop size from agricultural nozzles". New York, Atomization and Sprays, Vol. 24.

[14] Dabiri, S., et al., 2008, "Disintegration of moving liquid sheets using viscous potential analysis". USA: University of California.

[15] Lin, S. P., 2003, "Breakup of liquid sheets and jets", Cambridge University Press.

[16] Johnson, Ch. R., and Hansen, Ch. D., 2005, "The Visualization Handbook". Salt Lake City: University of Utah.

[17] Ashgriz, N., and SpringerLink (Online service), 2011, "Handbook of atomization and sprays: Theory and applications," Springer, New York, pp. xvi, 935 p.

[18] Nakayama, Y., and Aoki, K., 2001, "Progress of Visualization". Journal of visualization, Vol. 4.1, pp 9-18.

[19] Pavelek, M., Janotková, E. a Štětina, J., 2007, "Vizualizační a optické měřící metody". [Online] http://ottp.fme.vutbr.cz/users/pavelek/optika/.

[20] "TSI – Precision Measurement Instruments", [Online], http://www.tsi.com/.

[21] "Realisticky.cz" Krynický Martin, [Online], http://www.realisticky.cz/.

[22] Smits, A. J., and Lim, T. T., 2003, "Flow Visualization: Techniques and examples", London: Imperial College Press. ISBN 1-86094-193-1.

[23] Hulst, H. C., and H.C. Van De Hulst. 1957, "Light scattering by small particles". Courier Corporation.

[24] "The Electronic Universe", Dr. Greg Bothun, University of Oregon, [Online], http://zebu.uoregon.edu/2004/ph311/lec16.html.

[25] Držata, M., 2014, "Rigorózní simulace interakce světla s buňkami". Bakalářská práce, Vysoké Učení Technické v Brně, Brno.

[26] Ďurdina, L., 2010, "Metody vizualizace proudění", Bakalářská práce, Vysoké učení technické v Brně, Brno.

[27] Sridhara, S. N., and Raghunandan, B. N., 2010, "Photographic investigation of jet disintegration in airblast sprays". JAFM, Vol. 3, No. 2, pp. 111-123.

[28] Lee, E. J., Oh, S. Y., Kim, H. Y., James, S. C., and Yoon, S. S., 2010, "Measuring air core characteristics of a pressure-swirl atomizer via a transparent acrylic nozzle at various Reynold numbers". Experimental Thermal and Fluid Science, Vol. 34, pp. 1574-1483.

[29] Berrocal E., et al., 2008, "Application of structured illumination for multiple scattering suppression in planar laser imaging of dense sprays". Optics Express. Vol. 16.22, pp.17870-17881.

[30] Kristensson, E., 2012, "Structured Laser Illumination Planar Imaging SLIPI Applications for Spray Diagnostins". Ph.D Thesis. Lund University.

[31] Ďurdina, L, Jedelský, J., and Jícha, M., 2012, "Spray structure of a pressure-swirl atomizer for combustion applications" EPJ web of conferences, Vol. 25, EDP Sciences.

[32] Uruba, V., "Optické metody využívající změn hustoty media". Ústav termomechaniky AV ČR.

[33] "Photron", [Online], http://www.photron.com/.

[34] "FyzWeb", [Online], http://fyzweb.cz/clanky/index.php?id=111.

[35] Wang, D., Ma, Z., and Jeng, S., 1999, "Experimental study on large-scale simplex nozzle", California, AIAA, Vol. 35.

[36] Feggeler, D., Landwehr, F., and Walzel, P., 2006, "Experimantal investigation of sheet parameters vis PIV – comparison of different in practice, most commonly used nozzle geometries", Japan, ICLASS

[37] Adrian, R. J., 1991, "Particle-Imaging Techniques For Experimental Fluid Mechanics". Annual review of fluid mechanics, Vol. 23.1, pp. 261-304.

[38] "Dantec Dynamics". [Online], http://www.dantecdynamics.com.

[39] Schultz, C. and Sick, V., 2005, "Tracer-LIF diagnostics: quantitative measurement of fuel concentration, temperature and fuel/air ratio in practical combustion systems". Progress in Energy and Combustion Science, Vol.31.1, pp. 75-121.

[40] "CCD and CMOS sensor technology", Axis communications, [Online], http://www.axis.com/files/whitepaper/wp_ccd_cmos_40722_en_1010_lo.pdf.

[41] Litwillwer, D., 2001, "CCD vs. CMOS: Facts and Fiction". Photonics spectra , [Online]. Laurin Publishing Co. Inc.

[42] Schneider, B., and Wighley, G., 2010, "Diagnostics in Experimental Combustion Research". [PP presentation].

[43] "American lighting association", Michael Estrin, [Online], https://www.american lightingassoc.com/.

[44] Raffel, M., Willert, C., and Kompenhans, J., 1998, "Particle Image Velocimetry: A Practical Guide". Berlin: Mercedesdruck. ISBN 3-540-63683-8.

[45] Settles, G. S. 2001, "Schlieren and Schadowgraph Techniques: Visualizing Phenomena in Transparent Media". Germany. ISBN 3-540-66155-7.

[46] Leick, P., 2015, "Imaging Techniques", Atomization and Sprays, Darmstadt.

[47] Jedelský, J., Malý, M., Holub, M. and Jícha, M., 2015, "Some aspect of disintegration of annular liquid sheet in pressure-swirl atomization". Conference on Modelling Fluid Flow. Budapest.

[48] "The MartyBugs.net", Martin Pot, [Online], http://martybugs.net/.

[49] "Expert Reviews", Julie Price, [Online], http://martybugs.net/.

[50] Chen, S. K., Lefebvre, A. H. and Rollbuhler, J., 1992, "Factors influencing the effective spray cone angle of pressure-swirl atomizers", Journal of Engineering for gas turbines and power, Vol. 114.1, pp. 97-103.

List of symbols

Roman symbols

A	Surface area	$[m^2]$
b_p	Width of the inlet tangential port	[m]
c	Speed of light in vacuum	[m/s]
D	Droplet diameter	[m]
d_c	Width/diameter of the swirl chamber	[m]
d_o	Diameter of the exit orifice	[m]
d_s	Diameter of the spill-line orifice	[m]
E_A	Surface energy	[J]
F	Force along the fluid surface	[N]
f	Frequency of light	[Hz]
h_c	Height of the swirl chamber	[m]
h_p	Height of the inlet tangential port	[m]
l	Length of the fluid surface	[m]
l_o	Length of the exit orifice	[m]
l_p	Length of the inlet tangential port	[m]
m	Liquid mass	[kg]
n	Index of refraction	[-]
Δp	Inlet pressure differential	[Pa]
r	Droplet radius	[m]
r_c	Radius of the swirl chamber	[m]
U_0	Droplet velocity before a collision	[m/s]
V	Liquid volume	$[m^3]$
v	Speed of light in medium	[m/s]
We	Weber number	[-]

Greek symbols

α	Angle of the incident light ray	[deg]
β	Angle of the transmitted light ray	[deg]

λ	Wavelength	[m]
μ	Dynamic viscosity	[Pa·s]
ν	Kinematic viscosity	[m^2/s]
ρ_l	Liquid density	[kg/m^3]
σ	Surface tension	[kg/s^2]
τ	Shear stress	[Pa]
χ	Size parameter	[-]

Abbreviations

CCD	Charge Coupled Device
CMOS	Complementary Metal-oxide Semiconductor
PLI	Planar laser imaging
PLIF	Planar laser induced fluorescence
PIV	Particle image velocity
PS	Pressure-swirl
RMS	Root mean square
SCA	Spray cone angle
WIFI	Wireless fidelity